

Serveur Académique Lausannois SERVAL serval.unil.ch

Author Manuscript

Faculty of Biology and Medicine Publication

This paper has been peer-reviewed but does not include the final publisher proof-corrections or journal pagination.

Published in final edited form as:

Title: SHP-1 phosphatase activity counteracts increased T cell receptor affinity.

Authors: Hebeisen M, Baitsch L, Presotto D, Baumgaertner P, Romero P, Michielin O, Speiser DE, Rufer N

Journal: The Journal of clinical investigation

Year: 2013 Mar

Volume: 123

Issue: 3

Pages: 1044-56

DOI: 10.1172/JCI65325

In the absence of a copyright statement, users should assume that standard copyright protection applies, unless the article contains an explicit statement to the contrary. In case of doubt, contact the journal publisher to verify the copyright status of an article.

SHP-1 phosphatase activity counteracts increased T cell receptor affinity

Michael Hebeisen¹, Lukas Baitsch^{2,*§}, Danilo Presotto^{1,*}, Petra Baumgaertner², Pedro Romero², Olivier Michielin^{1,2}, Daniel E. Speiser² and Nathalie Rufer^{1,2}

¹Department of Oncology, Lausanne University Hospital Center and University of Lausanne, Lausanne, Switzerland

²Ludwig Center for Cancer Research, University of Lausanne, Lausanne, Switzerland

* These authors contributed equally to this work

§ Current address: Department of Cancer Biology, DANA-Farber Cancer Institute, and Department of Biological Chemistry and Molecular Pharmacology, Harvard Medical School, Boston, MA, USA

Address correspondence to: Nathalie Rufer, PhD, Ludwig Center for Cancer Research, University of Lausanne, c/o HO, niv 5, Avenue Pierre-Decker 4, CH-1011 Lausanne, Switzerland; phone: +41 21 314 01 99, fax: +41 21 314 74 77; e-mail: Nathalie.Rufer@unil.ch

Running title: Engineering of human CD8⁺ T cells with affinity-optimized TCRs

Word counts: 8577

Keywords: human, CD8 T cells, pMHC, TCR gene transfer, affinity, TCR signaling, gene expression, activatory/inhibitory receptors, PD-1, SHP-1, miR-155, miR-181a

Abbreviations: pMHC, peptide-MHC; WT, wild type; SSG, sodium stibogluconate

The authors have declared that no conflict of interest exists.

ABSTRACT

Anti-self/tumor T cell function can be improved by increasing TCR-peptide MHC (pMHC) affinity within physiological limits, but paradoxically further increases ($K_D < 1\mu\text{M}$) lead to drastic functional declines. Using human CD8^+ T cells engineered with TCRs of incremental affinity for the tumor antigen HLA-A2/NY-ESO-1, we investigated the molecular mechanisms underlying this high affinity-associated loss of function. As compared with cells expressing TCR affinities generating optimal function (K_D ; 5 to 1 μM), those with supraphysiological affinity (K_D ; 1 μM to 15 nM) showed impaired gene expression, signaling and surface expression of activatory/costimulatory receptors. Preferential expression of the inhibitory receptor programmed cell death-1 (PD-1) was limited to T cells with the highest TCR affinity, correlating with full functional recovery upon PD-L1 blockade. In contrast, upregulation of the Src homology 2 domain-containing phosphatase 1 (SHP-1/PTPN6) was broad, with gradually enhanced expression in CD8^+ T cells with increasing TCR affinities. Consequently, pharmacological inhibition of SHP-1 with sodium stibogluconate augmented the function of all engineered T cells, and this correlated with the TCR affinity-dependent levels of SHP-1. These data highlight an unexpected and global role of SHP-1 in regulating CD8^+ T cell activation and responsiveness, and support the development of therapies inhibiting protein tyrosine phosphatases to enhance T cell mediated immunity.

INTRODUCTION

CD8⁺ T cell responses rely on the specific recognition by T cell receptors (TCRs) of small immunogenic peptides presented in the context of MHC class I molecules at the surface of infected or transformed cells. Binding of TCR to peptide-MHC is characterized by relatively low molecular affinity (100 μ M to 1 μ M) and high specificity and sensitivity, thus enabling T cells to detect rare antigenic epitopes on antigen presenting cells (APC) (1). Due to mechanisms of central and peripheral tolerance, circulating autoreactive T cells recognizing self/tumor associated antigens typically have TCR-pMHC affinities at the lower end of the physiological range and/or are maintained in unresponsive functional states when compared with pathogen Ag-specific T cells. This might in part explain why tumor-reactive T cell responses detected in cancer patients often fail to control or eliminate advanced disease (2).

Adoptive cell transfer (ACT) of T cells engineered to express TCRs of increased affinity for tumor antigens represents an attractive immunotherapeutic approach to induce and boost immune reactivity toward poor immunogenic tumors (3). Numerous studies suggest that enhancing TCR-pMHC interactions (half-life and affinity) would endow T cells with higher functional and protective capacity (4). However, it was also shown that T cells engineered with TCR of very high supraphysiological affinity for pMHC ($K_D < 1$ nM) lose antigen specificity and become cross-reactive or alloreactive (5-7). As such, TCR optimization through affinity alterations has to include the careful evaluation of optimal T cell responsiveness, to ensure the safety of TCR-engineered T cells in clinical trials (3).

Recently, we characterized the functional impact of TCR-pMHC binding strength by using a panel of human CD8⁺ T cells engineered through structure-based rationally-designed TCRs of incremental affinity for the self/tumor antigen A2/NY-ESO-1₁₅₇₋₁₆₅ (8-11). At low peptide dose stimulation, T cells with TCR affinities ranging in the upper physiological limit (K_D from 5 μ M to 1 μ M) display higher biological responses, when compared with T cells expressing the wild-type (WT) TCR (K_D at 21.4 μ M) (11). Strikingly, tumor-reactive T cells expressing TCRs of supraphysiological affinities (K_D from 1 μ M to 15 nM) show drastic functional decline irrespective of CD8 co-engagement, which is not associated with loss of antigen specificity (11). Similarly, other studies reported that T cells with TCR-pMHC affinities and/or half-lives extending above the natural range exhibit attenuated T cell activation upon TCR triggering, as well as impaired expansion potential and responsiveness (12-16).

To identify the molecular mechanisms underlying these functional defects, we characterized global gene expression, signaling pathways and activatory/inhibitory membrane receptors on human CD8⁺ T cells engineered with TCRs of incremental affinity for HLA-A2/NY-ESO-1. We describe how the inhibitory receptor PD-1 and the Src homology 2 domain-containing phosphatase 1 (SHP-1) are involved in restricting T cell function in TCR-engineered CD8⁺ T cells. Strikingly, SHP-1 mediated a gradual functional inhibition of CD8⁺ T cells, along TCR binding affinity, independently of PD-1 involvement. Together, these data indicate that, in the context of adoptive cell therapy, TCR-mediated SHP-1 signaling may counter regulate T cell responses, by limiting the potential cytotoxic effect of TCR-optimized CD8⁺ T cells against self/tumor antigens.

RESULTS

Impaired function of human primary CD8⁺ T cells expressing self/tumor-specific TCRs of supraphysiological affinity

Using a panel of affinity-optimized HLA-A*0201-restricted NY-ESO-1₁₅₇₋₁₆₅-specific TCR (BC1) variants with gradually increased affinity of up to 1400-fold from the native TCR (Supplemental Table 1; (8, 9)), we previously found that maximal biological activity occurred within a well-defined affinity window with K_D ranging from 5 to 1 μ M (10, 11). Importantly, under low peptide stimulation conditions, cellular activity, including Ca^{2+} mobilization capacity (Figure 1A) and tumor cell killing (Figure 1B), was globally attenuated for T cells expressing either TCRs of very low ($K_D > 100 \mu$ M; V49I) or of supraphysiological ($K_D < 1 \mu$ M; TM α , QM α and wtc51m) affinities. Conversely, high concentrations of NY-ESO-1₁₅₇₋₁₆₅ peptide loaded on APCs restored the Ca^{2+} mobilization capacity of CD8 T cells with supraphysiological TCRs (Supplemental Figure 1), consistent with our recent report (11). Similar data were obtained independently of stimulation with peptide-pulsed APCs or A2/peptide multimers. This functional decline was not caused by lower TCR expression as engineered CD8⁺ T cells and α -TCR knockout SUP-T1 cells expressed comparable surface levels of TCR β chain (BV13.1) and of overall TCR $\alpha\beta$ chains (Figure 1C, Supplemental Figure 2A).

Upon short-term peptide stimulation, we observed substantial TCR down-regulation (reduced multimer fluorescence; Figure 1E) in all engineered CD8⁺ T cells independently of their TCR affinities (e.g. optimal versus supraphysiological). TCR down-modulation was assessed either by multimer fluorescence (Figure 1E) or by staining with an anti-BV13 mAbs (Supplemental Figure 2). In contrast, reduced CD8

co-receptor expression (Figure 1D; Supplemental Figure 2) was primarily found in T cells expressing TCRs mediating maximal/optimal function (A97L, DM β , TM β) rather than in T cells of supraphysiological TCR affinity (TM α , wtc51m). Altogether, our data further emphasize the paradoxical status of these NY-ESO-1 specific T cells expressing very high TCR affinities with impaired functionality despite retaining robust surface binding TCR avidity and TCR down-regulation capacity upon stimulation (Figure 1, (10, 11)). These findings suggest the presence of potential mechanisms controlling T cell activation, signaling and subsequent functionality.

Altered gene expression profiles in CD8⁺ T cells with TCRs of supraphysiological affinity following antigen-specific stimulation

In order to uncover the molecular mechanisms involved in the impaired functional responsiveness of cells bearing supraphysiological TCRs, we performed a genome-wide microarray analysis on primary CD8⁺ T cells expressing the panel of TCR variants following low dose of A2/NY-ESO-1 specific multimer stimulation (Figure 2A). We compared the global gene expression levels of all samples before and after 6 hours of stimulation, and found 538 gene probes showing at least a two-fold differential expression (data not shown). Similar gene expression patterns were observed between engineered T cells belonging to the same culture conditions (unstimulated versus 6 hr-stimulated), and could accordingly be defined within two distinct clusters or profiles. However, unsupervised hierarchical clustering revealed that the 6 hr-stimulated T cells expressing infra- (V49I) and supra-physiological (wtc51m) affinity TCRs both clustered with the unstimulated T cells (Figure 2A).

To obtain a gene signature of optimal T cell activation, we compared the gene expression profiles of the four TCR-transduced CD8⁺ T cells known to produce maximal function (G50A, A97L, DMβ, TMβ) before and after 6 hr activation. With this strategy, we identified 524 differentially expressed genes and classified them according to six general Gene Ontology (GO) terms. The average absolute log₂ fold change (0 to 6 hr) of the genes within each GO term is represented in Figure 2B. Remarkably, all GO terms (immune response, T cell activation, cell proliferation, signaling, gene expression and apoptosis) had the same overall outline demonstrating a drastic under-representation of the gene expression within V49I and wtc51m TCR variants. The average absolute fold change was progressively increased from low to optimal TCR affinity, before declining in T cells with supraphysiological TCR variants (TMα and wtc51m). Interestingly, the pattern of gene expression profile related to apoptosis strongly correlated to the one observed following A2/peptide multimer stimulation and staining with Annexin-V (11), with highest levels of apoptosis for CD8⁺ T cells expressing optimal TCRs. In addition, several key genes involved in T cell activation (e.g. *CRTAM*, *IFNG* and *IL2RA*) as well as costimulatory molecules (e.g. *TNFRSF18*, *TNFRSF4*, *TNFRSF9*) showed a 2-fold or greater change, and displayed the same overall bell-shape profile following 6h-stimulation (Figure 2C). No major changes in genes classified to the GO terms were observed at baseline in un-stimulated CD8⁺ T cells (Supplemental Figure 3).

Similar to the functional data (Figure 1), gene expression analyses revealed that T cells engineered with TCR of infra- or supra-physiological affinity clustered together and failed to properly modulate their transcriptome upon specific TCR triggering. Conversely, the transcriptional gene signatures of CD8⁺ T cells expressing optimal TCR variants (G50A, A97L, DMβ and TMβ) revealed drastic global changes (up- or

down-regulation) in gene expression levels following short-term antigen-specific stimulation, supporting enhanced T cell responsiveness.

Affinity of TCR-pMHC interaction impacts on the intensity and duration of TCR-mediated intracellular signaling

To gain functional insights into the molecular mechanisms underlying altered gene expression profiling associated with very low or very high TCR affinities (Figure 2), we explored the impact of TCR affinity on cell signaling. We assessed the activation levels of ZAP-70, a proximal activatory molecule of TCR signaling and of the distal MAPK family members ERK1/2 (p38). SUP-T1 and CD8⁺ T cells expressing TCR variants were stimulated with A2/NY-ESO-1-specific multimers and levels of phosphorylated ZAP-70 (pY319) and ERK1/2 (pT202/pY204 ERK1; pT185/pY187 ERK2) were quantified in kinetic analyses. Upon specific stimulation, we found differential levels of ZAP-70 phosphorylation intensity and duration correlating with TCR affinity variants (Figure 3, Supplemental Figure 4). V49I-transduced T cells showed only transient and low levels of ZAP-70 phosphorylation, whereas cells expressing TCR variants mediating optimal functions (e.g. A97L, DM β) generated fast and sustained ZAP-70 phosphorylation. Importantly, in CD8⁺ (Figure 3C, Supplemental Figure 4) and SUP-T1 (Figure 3, A and B) cells expressing supraphysiological TCR affinities (e.g. QM α and wtc51m), ZAP-70 phosphorylation declined rapidly and substantially following specific stimulation.

ERK1/2 phosphorylation profiles corresponded with those observed for ZAP-70 phosphorylation, with an overall increase in the signaling intensities depending as well on the TCR affinity variants. Maximal phosphorylation was found for TCR

variants of optimal function, while T cells with supraphysiological TCRs showed mostly a transient and rapid loss of ERK1/2 phosphorylation following TCR stimulation (Figure 3, Supplemental Figure 4). Together, the transgenic TCR affinity strongly impacted on both the intensity and the duration of ZAP-70 and ERK1/2 phosphorylations. Importantly, CD8⁺ T cells expressing supraphysiological TCRs affinity presented a drastically reduced activation of key TCR downstream signaling pathways (Ca²⁺ and MAPK), and this occurred at a very proximal step in the TCR signaling cascade (ZAP-70). Conversely, the low cell signaling observed in V49I-expressing T cells nicely correlated with the poor intrinsic binding avidity of this particular TCR (10, 11).

Impact of TCR-pMHC affinity on the expression of co-activatory/inhibitory receptors

Since global genome profiling revealed reduced expression of genes involved in costimulatory/activatory molecules in supraphysiological T cells (Figure 2), we next focused on measuring the surface expression levels of CD28, as well as CD27 and HVEM and their respective ligands (CD70 and BTLA) (Figure 4A). Under steady-state conditions, most of the TCR transduced CD8⁺ T cells, including cells with the lowest TCR-affinity variant (V49I) expressed similar levels of CD28, as well as of CD27 and HVEM with their respective ligands. Strikingly, T cells bearing supraphysiological TCR affinity (wtc51m) had statistically significant lower expression of CD28, HVEM and CD70, all three involved in T cell activation signaling. In contrast, BTLA, known to inhibit T cell function (17), was expressed at the highest levels in wtc51m-expressing T cells (Figure 4A). No significant differences in CD8 α expression were found (data not shown), yet there was a trend of lower expression of the CD8 β in T cells with supraphysiological TCRs (Figure 4A).

Significantly reduced expression of Granzyme B and Perforin (Figure 4B) was also found in the latter T cells (wtc51m), consistent with their attenuated killing capacities (Figure 1B). Importantly, similar data were obtained when CD8⁺ T cells were stimulated with A2/NY-ESO-1-specific multimers over a 24 hr- and 48 hr-period of time (data not shown). Overall, these data further support the notion that CD8⁺ T cells expressing supraphysiological TCR affinities likely exhibit molecular mechanisms that actively down-regulate surface co-activatory molecules/receptors. This was readily observed under steady-state conditions.

Engineered T cells of supraphysiological TCR affinity show enhanced expression of PD-1 correlating with full functional recovery upon PD-L1 blockage

CD8⁺ T cells express multiple negative regulators, such as BTLA, PD-1 and CTLA-4, which have been proposed to play central roles in preventing uncontrolled T cell activation and autoimmunity during inflammatory responses (18). Therefore, we sought to determine whether PD-1 could functionally regulate CD8⁺ T cells expressing TCRs of increased affinities. We assessed PD-1 expression in unstimulated TCR engineered T cells (Figure 5, B and C). Comparable with mRNA data (Figure 5A), elevated PD-1 levels were exclusively found in CD8⁺ T cells of highest supraphysiological affinity (wtc51m). Of note, *PDI* mRNA fold-change at 6 hr stimulation showed the same overall bell-shape profile with maximal expression in T cells mediating optimal function (A97L, DM β and TM β), thereby indicating that PD-1 expression can also be induced shortly after antigen-specific TCR stimulation (Figure 5A). No significant differences were found in expression levels of PD-1 ligand PD-L1 (Figure 5B) and CTLA-4 (data not shown).

Since PD-L1 surface expression was highly comparable across the TCR affinity panel, we next evaluated the biological significance of PD-1 expression on T cell responsiveness by blocking PD-1/PD-L1 interaction. All transduced CD8⁺ T cells were incubated with PD-L1 neutralizing antibody prior to LAMP1/CD107a degranulation assays (Figure 5, D and E). After 4 hr triggering with the NY-ESO-1 peptide, PD-L1 blockade had no effect on the CD107a degranulation in most of CD8⁺ T cells, with the exception of the supraphysiological TCR variant (wtc51m) that exhibited an increased proportion of degranulating cells, even reaching similar levels to the other TCR variants (Figure 5D). Relative CD107a degranulation activity further confirmed that blocking the PD-1/PD-L1 pathway led to full functional recovery in the supraphysiological T cells (Figure 5E). Collectively, our data revealed preferential expression of PD-1 in supraphysiological CD8⁺ T cells, i.e. those with TCRs in the nanomolar range (wtc51m). Furthermore, PD-L1 blockade restored CD107a degranulation in PD-1^{high} expressing cells, demonstrating its key implication in the functional regulation of those T cells.

Enhanced expression of SHP-1 phosphatase in a TCR-affinity dependent manner

SHP-1 and SHP-2 phosphatases can be recruited by multiple inhibitory surface receptors in T cells, and inhibit TCR signaling (19), through dephosphorylation of proximal signaling targets (e.g. LCK, ZAP-70, CD3 ζ). Under un-stimulated conditions, *SHPI* gene expression was progressively increased from low to high TCR affinity (Figure 6A; baseline). We characterized the expression levels of total SHP-1 protein and its phosphorylated activatory form Y536 (20) as well as of total SHP-2 protein (Figure 6, Supplemental Figure 5). Maximum levels of SHP-1 phosphorylation were detected in both CD8⁺ and SUP-T1 T cells transduced with

supraphysiological TCR variants (e.g. QM α and wtc51m) after antigen-specific stimulation, and already under steady-state conditions. Importantly, transient levels of phosphorylated SHP-1 were also enhanced in the other TCR variants upon stimulation, yet never reached those observed in QM α and wtc51m-transduced T cells. Total SHP-1 protein revealed expression patterns that followed the same TCR binding hierarchy, with intermediate and highest levels found for optimal and supraphysiological TCR affinities, respectively (Figure 6). In CD8⁺ T cells, the weak binding TCR ligand V49I was also able to trigger SHP-1 protein expression and phosphorylation, consistent with a previous report (21) showing that SHP-1 is involved in antagonist-mediated inhibition. Thus, differing to PD-1 expression, SHP-1 phosphatase was found up-regulated in a TCR affinity-dependent manner with substantial expression levels readily found in T cells of optimal TCRs affinities. A comparable trend was observed for total SHP-2 expression (Supplemental Figure 5).

Finally, we assessed the expression levels of miR-181a and miR-155 (Figure 6E), two micro RNA, mostly known to impact, respectively, on lymphocyte development and function (22, 23). Following specific TCR stimulation, only minor changes in miR-181a expression were found within the engineered panel of CD8⁺ T cells. This highly contrasted with the strong induction in pri-miR-155 (BIC transcript) and miR-155 expression observed within T cells expressing WT and optimal TCR affinities (e.g. A97L, DM β).

Impact of pharmacological SHP-1 phosphatase inhibition on degranulation and cytotoxicity of TCR engineered CD8⁺ T cells.

Sodium stibogluconate (SSG) is widely used to treat visceral leishmaniasis and was recently identified as an important clinically suitable protein tyrosine phosphatase inhibitor in cancer patients (24, 25). Notably, SSG has been shown to selectively inhibit protein tyrosine phosphatases, among which SHP-1 was the most sensitive (26). Given the elevated levels of SHP-1 and SHP-2 protein expression within engineered CD8⁺ T cells, we next examined whether SSG treatment might improve their function, irrespectively of PD-1 expression (Figure 7). We incubated the CD8⁺ T cells in the presence or absence of SSG for 3 days, at a concentration (50 µg/ml) shown to partially inhibit SHP-2 activity as well (26). Following pharmacological inhibition of SHP-1/SHP-2, increased degranulation potential (Figure 7, A and B) was found within the whole T cell panel, except for cells expressing the infra-physiological TCR affinity V49I. Importantly, functional recovery was further validated in target cell killing experiments (Figure 7, C and D), and correlated well with the affinity-dependent levels of SHP-1 phosphatase found in T cells. Indeed, and in agreement with their stronger phosphorylation levels, supraphysiological T cells showed better killing recovery capacity than compared to WT and optimal T cells. Although we cannot formally exclude off-target effects of SSG treatment, these results support the notion that SHP-1 phosphatase (and eventually SHP-2) may mediate a gradual functional inhibition in TCR-engineered CD8⁺ T cells, depending on TCR affinity, but not necessarily on the degree of PD-1 involvement.

DISCUSSION

The panel of rationally designed NY-ESO-1₁₅₇₋₁₆₅-specific TCRs with incremental affinity (8, 9) provides a unique model to investigate the relationship between TCR affinity and T cell function, as well as its modulation by activatory/inhibitory co-receptors and their signaling pathways. Here, we show that the impaired functionality recently observed in CD8⁺ T cells engineered with supraphysiological TCR affinities ($K_D < 1 \mu\text{M}$) (11) was associated with a strong decrease in overall gene expression profile, intracellular signaling and surface expression of activatory TNFR superfamily members (Figures 2 to 4). Our major findings revealed that the T cell effectiveness of engineered CD8⁺ T cells was limited by at least two mechanisms. The first one was characterized by the preferential expression of PD-1 inhibitory receptor within T cells of highest supraphysiological TCR affinity (wtc51m variant), and this correlated in those cells with restored cell responsiveness upon PD-1/PD-L1 blockade (Figure 5). The second one was associated with the gradual increased expression of SHP-1 phosphatase in a TCR affinity-dependent manner, from WT to very high TCR affinities (Figure 6). In contrast to PD-1/PD-L1 blockade experiments, pharmacological inhibition using sodium stibogluconate known to inhibit SHP-1 (and partially SHP-2) allowed further incremental gaining of cell function in engineered CD8⁺ T cells, according to their TCR binding affinity (Figure 7).

Adoptive cell therapy (ACT) using autologous T lymphocytes reprogrammed by TCR gene transfer aims to confer robust immune reactivity towards defined tumor-associated antigen-bearing cells to which the endogenous T cell repertoire is weak or non-responsive. Recently, two clinical trials were conducted whereby autologous T cells transduced with affinity-enhanced TCRs specific for tumor-associated antigens

were adoptively transferred to patients with metastatic melanoma or sarcoma, and demonstrated objective clinical responses (27, 28). Robbins and colleagues (28) were the first to examine the in vivo efficacy of adoptively transferred autologous T cells transduced with the sequence-optimized 1G4 TCR specific for NY-ESO-1₁₅₇₋₁₆₅. This genetically modified TCR possesses an affinity that lies just beyond the natural affinity range and confers maximal in vitro functionality with lowest cross-reactivity (6). In line with these observations, vaccination with peptide ligands of intermediate affinity yielded the most potent tumor-reactive CD8⁺ T cells in vivo, and best tumor growth control in BALB/c mice (15). Recently, Corse et al. further confirmed that peptide binding to the TCR with medium strength induced optimal in vivo CD4⁺ T cell activation and subsequent immune responses (12). Future directions involve integrating the vast knowledge acquired from the in vitro experimental studies into the context of in vivo immune responses and clinical trials of adoptive cell therapy (reviewed in (29)).

The in silico structure-based approach allowed to rationally design sequence substitutions in the CDR2 α and/or CDR2 β and/or CDR3 β loops, known to interact either with the MHC surface or the bound peptide (Supplemental Table 1; (8, 9), Zoete V., Irving M., and Michielin O., *unpublished observations*). We also included in this panel, the supraphysiological TCR variant wtc51m, previously identified by phage-display screening, with nanomolar range of affinity to the HLA-A2/NY-ESO-1 complex (30). Importantly, and despite their impaired functionality, all engineered CD8⁺ T cells expressing supraphysiological TCRs of $K_D < 1 \mu\text{M}$ (TM α , QM α and wtc51m) retained a high degree of specificity towards the cognate pMHC target in functional assays (10, 11). An important finding in this study is that, only engineered T cells with the highest TCR affinity variant (wtc51m) up-regulated inhibitory

receptors (PD-1 and BTLA) and conversely down-regulated co-activatory receptors (CD28, HVEM, CD8 β) (Figure 4 and 5). What remains intriguing is how such affine T cells control the expression of their activatory/inhibitory receptors readily under steady-state settings. One likely explanation is that, in contrast to the rational design approach ((8, 9), Zoete V., Irving M., and Michielin O., *unpublished observations*), gain in affinity for the wtc51m TCR variant resulted from multiple increased interactions with the HLA-A2 molecule, as this particular TCR contained up to four amino acid replacements within the CDR2 β loop (30). Besides that, TCR surface expression also integrates and potentiates the effects of several variables/parameters including multiple coreceptors, TCR density, multivalent TCR clustering, and basal T cell activation state (reviewed in (4)). Together, weak but continuous TCR-A2 specific interactions regardless of the nature of the bound peptide, may occur during the in vitro culture and periodic expansion of the transduced primary CD8⁺ T cells and SUP-T1 cells (both HLA-A2 positive) and may be sufficient to modulate activatory/inhibitory receptor expression already under resting culture conditions. Notably, these conditions are very similar to the in vitro culture of autologous T cells transduced to express TCRs against HLA-A2/tumor antigens and further expanded before ACT (28). Collectively, these data emphasize the potential impact of TCR-A2 binding affinity in relation to membrane receptor expression, T cell activation, and signaling, and highlight the need to carefully assess TCR affinity/avidity in relation to its functional efficacy for optimizing the design of ACT and vaccination.

An important aspect is to understand how T cells sense the differences in the strength of TCR-peptide/MHC interactions, as observed here within the panel of affinity-optimized T cells. One of the current models (defined as the productive hit rate model) postulates that TCR-pMHC binding interactions need to be sufficiently long

to initiate productive TCR signaling and subsequent T cell activation (reviewed in (31)). It also integrates that TCR-pMHC bonds must be released quickly enough to enable serial triggering, to acquire strong signals upon multiple interactions between TCRs and the pMHC complex. As a consequence, the productive hit rate model proposes that very fast or very slow TCR-pMHC dissociation rates would reduce the activation potential of T lymphocytes (14). The findings that maximal function occurred within a well-defined affinity window (K_D ; 5 to 1 μ M), and that above it, T cells engineered with supraphysiological TCR affinities responded less efficiently to antigen stimulation further support this model (11). Importantly, recent *in vivo* studies show that functional T cell responses are also largely influenced by the TCR ligand affinity/avidity and the amount of presented antigen (12, 32). These observations are compatible with the notion that T cell clonotypes with a broad range of TCR affinities/avidities may participate equally (codominantly) in immune responses, and that this may depend both on peptide-MHC potency and density (33).

Beside the biophysical regulation imposed by the TCR-pMHC binding parameters, the recruitment of inhibitory receptors like PD-1 (programmed death-1) in tumor-specific T cells of supraphysiological TCR affinity (wtc51m) reveals the presence of an additional level of control allowing to restrain effector function in those cells, such as observed in autoimmune or anti-tumoral responses. Engagement of PD-1 by PD-1 ligand 1 (PD-L1) is thought to be critical in preventing activation of self-reactive T cells that have escaped thymic clonal deletion (18). Accordingly, PD-1-deficient mice spontaneously develop autoimmune diseases (34), while in humans a regulatory polymorphism in PD-1 is associated with susceptibility to systemic lupus erythematosus and multiple sclerosis (35, 36). Induction of PD-L1 ligand expression has also been described in various tumor cells as a mechanism of cancer immune

evasion (2). Furthermore, PD-1 expression is inducible in T cells following TCR stimulation, and may be involved in the suppression of T cell activation in vitro and in vivo (37). However, the molecular basis by which PD-1 inhibits T cell activation is not fully understood. A recent study by Yokosuka and colleagues showed that upon PD-L1 binding, ITIM-containing PD-1 could directly inhibit TCR-mediated signaling by recruiting SHP-2 phosphatase (38).

SHP-1 phosphatase negatively regulates TCR signal transduction and T cell activation upon TCR engagement, and contributes to the setting of thresholds during thymocyte selection (19). Recently, SHP-1 was shown to limit the production of virus-specific effector CD8 T cells without impacting the formation of long-lived central memory cells (39). Furthermore, abrogation of SHP-1 expression in tumor-specific T cells improved efficacy of adoptive immunotherapy by enhancing the effector function and accumulation of short-lived effector T cells in vivo (40). Here, we extend these findings by showing that SHP-1 phosphatase may represent an important regulatory molecule in CD8⁺ T cells engineered with incremental affinity TCR variants. Importantly, SHP-1 was found upregulated in a TCR affinity-dependent manner with the highest levels in T cells with supraphysiological TCRs (Figure 6, Supplemental Figure 5). This suggests that SHP-1 may play a dual role and restricts not only T cell signaling at the very low range of TCR stimulation (e.g. with antagonist ligands) as previously described (21), but also at the higher range (e.g. with optimized and supraphysiological TCR affinity ligands). Our observations are further consistent with a recent study showing that B cell receptor (BCR) signaling was limited by SHP-1 activity in the most proliferating germinal center B cells, revealing a regulatory effect on the affinity-based selection of those cells (41). However, additional studies using SHP-1-specific small interfering RNA are still

needed to fully demonstrate the impact of SHP-1 in mediating functional inhibition of affinity-optimized T cells.

Specific microRNAs have been shown to be critical for T cell development and function. For instance, transcriptional activation of miR-155 is detectable upon lymphocyte activation (42) and correlates with increased expression in human antigen-experienced CD8⁺ T cell subsets (23). Here we provide evidence that miR-155 expression, but paradoxically not miR-181a, may be involved in modulating T cell function in TCR affinity-optimized CD8⁺ T cells. Thus, it will be of great importance to further explore the mechanisms by which miR-155 may influence cell activation and responsiveness along the TCR affinity range in peripheral T lymphocytes.

CTLA-4 and PD-1 are two checkpoint inhibitory receptors that have become novel targets for treating cancer patients, as these molecules can be specifically blocked with antibodies (43). Consequently, antibodies against PD-1 and PD-L1 have entered phase 1 clinical trials, and initial results showing objective tumor regression are highly promising (44, 45). More recently, two phase 1 trials using the phosphatase inhibitor sodium stibogluconate (SSG) in combination with IFN- α 2b have demonstrated safety and targeted inhibition in cancer patients (24, 25). Our findings highlight the critical role of SHP-1 expression among the whole panel of engineered CD8⁺ T cells. In particular, we show that targeting SHP-1 in T cells with optimal antitumor-specific TCRs (A97L, DM β and TM β) further augment their functional efficacy. These observations provide the rational for adoptive T cell therapy using affinity-optimized TCR variants combined with treatments blocking PD-1 and/or SHP1/2 phosphatases.

METHODS

Cell lines and primary CD8⁺ T cells

TCR- α knockout SUP-T1 cells and HLA-A2⁺/TAP-deficient T2 cells were cultured in RPMI supplemented with 10% FCS, 10 mM Hepes, penicillin (100 U/ml) and streptomycin (100 μ g/ml). Human primary HLA-A2⁺ CD8⁺ T lymphocytes were obtained following positive enrichment using anti-CD8-coated magnetic microbeads (Myltenyi Biotec), and cultured in RPMI supplemented with 8% HS and 150 U/ml recombinant human IL-2. Cell surface analysis and functional assays were always performed between day 10 and 15 post stimulation with 30 Gy irradiated PBMC as feeder cells and 1 μ M PHA (Oxoid) as described before (10).

NY-ESO-1-specific TCR $\alpha\beta$ constructs, lentiviral production and cell transduction

Cloning strategies and lentiviral production were performed as described previously (10, 11). The full-length codon-optimized TCR AV23.1 and TCR BV13.1 chain sequences of a dominant NY-ESO-1₁₅₇₋₁₆₅-specific T cell clone of patient LAU 155 were cloned in the pRRL, third generation lentiviral vectors, as a hPGK-AV23.1-IRES-BV13.1 construct. Structure-based amino acid substitutions were introduced into the wild-type (WT) TCR sequence using the QuickChange mutagenesis kit (Stratagene) and confirmed by DNA sequencing. Supernatant of lentiviral transfected 293T cells were used to infect SUP-T1 or primary CD8⁺ T lymphocytes. PE-labeled A2/NY-ESO-1₁₅₇₋₁₆₅-specific multimers were used to sort transduced primary CD8⁺ T cells in order to enrich for multimer⁺ cells by flow cytometry (FACS Vantage SE machine; BD Biosciences). Integrated lentiviral copy number was relatively equivalent for each one of the TCR variants within each type of transduced cell; i.e.

8-10 lentivirus copies/genome of SUP-T1 cells and 1-2 copies/genome of CD8⁺ T cells, as described in (11).

Flow cytometry analysis

Levels of NY-ESO-1-specific BV13.1/AV23 TCR expression on SUP-T1 and CD8⁺ T cells were monitored with PE-labeled NY-ESO-1₁₅₇₋₁₆₅-specific multimers (TC Metrix), FITC-conjugated BV13.1 antibody (Beckman Coulter) and FITC-conjugated pan-TCR $\alpha\beta$ antibodies (Beckman Coulter) before each experiment as previously described (10). For CD8 and TCR down-regulation experiments, TCR-transduced CD8⁺ T cells were stimulated with 0.1 $\mu\text{g/ml}$ unlabeled HLA-A2/NY-ESO-1₅₇₋₁₆₅-specific multimers for 4 hours at 37°C, before staining with FITC-conjugated CD8 and PE-labeled A2/NY-ESO-1₁₅₇₋₁₆₅ multimers. The proportion (in %) of CD8⁺ T cells with reduced CD8 stainings as well as the mean fluorescence intensity (MFI) by multimer stainings was measured by flow cytometry (GalliosTM, Beckman Coulter). Staining of surface costimulatory molecules and co-activatory/inhibitory receptors was performed for 20 min at 4°C using the fluorophore-conjugated antibodies listed in Supplemental Methods. Intracellular stainings were performed according to the manufacturer's instructions. Data were acquired on a GalliosTM Flow Cytometer (Beckman Coulter) analyzed using FlowJoTM (TreeStar).

Calcium flux assays upon NY-ESO-1 multimer stimulation

5×10^4 TCR-transduced CD8⁺ T lymphocytes were loaded with 2 μM Indo 1-AM (Sigma-Aldrich) for 45 min at 37°C. Cells were washed and resuspended in 250 μl prewarmed RPMI containing 2% FCS. Baseline was recorded for 30 sec before 1

$\mu\text{g/ml}$ of unlabeled A2/NY-ESO-1 multimer was added to the cells. Intracellular Ca^{2+} flux was assessed during 5 min, under UV excitation and constant temperature of 37°C using a thermostat device on a LSR II SORP (BD Biosciences) flow cytometer. Indo-1(violet)/Indo-1(blue) 405/525 nm emission ratio was analyzed by FlowJo kinetics module software (TreeStar).

Chromium release assays

Specific antigen recognition lytic activity of the NY-ESO-1-specific CD8^+ T engineered with TCR variants of increased affinities was assessed functionally in 4 hours ^{51}Cr -release assays against the melanoma cell lines NA8 (HLA-A2⁺/NY-ESO-1⁻) as well as Me 275 and Me 290 (HLA-A2⁺/NY-ESO-1⁺). The percentage of specific lysis was calculated as follow: $100 \times (\text{experimental} - \text{spontaneous release})/(\text{total} - \text{spontaneous release})$.

Microarray analysis

Primary CD8^+ T cells (1×10^6) transduced with sequence-optimized NY-ESO-1-specific TCR variants were cultivated in RPMI supplemented with 8% HS and 10 U/ml rhIL-2 for 24 hours and left either unstimulated (baseline, 0 hr) or were stimulated with low dose $0.002 \mu\text{g/ml}$ unlabeled A2/NY-ESO-1₅₇₋₁₆₅-specific multimer for 6 hours at 37°C to avoid activation-induced cell death. The proportion of Annexin-V⁺ cells was $< 10\%$ (data not shown). After incubation, cells were washed with ice-cold PBS before quick freezing in liquid nitrogen. Frozen cell pellets were sent to Miltenyi Biotec GmbH and processed according to the vendor-recommended protocol for gene expression analysis as described in Supplemental

Methods. The gene expression data described in this manuscript have been deposited in the NCBI Gene Expression Omnibus and are accessible through the GEO accession number (GSE42922).

Western blot analysis

For all experiments, 1×10^6 untransduced or TCR-transduced SUP-T1 and primary CD8⁺ T cells were either left unstimulated (baseline) or stimulated with 10 $\mu\text{g/ml}$ unlabeled A2/NY-ESO-1₁₅₇₋₁₆₅ multimers for the indicated time in a 37°C water bath before washing with ice-cold PBS and quick freezing in liquid nitrogen. Following cell extraction, proteins were separated by SDS-PAGE and subsequently probed with the following primary antibodies: goat anti-SHP-1 (C-19) (LabForce AG), rabbit anti-pERK1/2 (Thr202/Tyr204) (D13.14.4E), mouse anti-ERK1/2 (3A7), rabbit anti-pZAP-70 (Tyr319)/Syk(Tyr352), rabbit anti-ZAP-70 (99F2) (Cell Signaling Technology), rabbit anti-pSHP-1 (Tyr536) (ECM Biosciences), mouse anti- α -tubulin (B-5-1-2) (Sigma-Aldrich) and rabbit anti-actin (AA20-33) (Sigma-Aldrich). Quantification of specific bands was done using PhosphoImager software ImageJ and normalized to α -tubulin or actin expression levels.

Quantitative PCR analysis for miR-155 and miR-181a expression

TCR-transduced CD8⁺ T cells (1×10^6) were left either unstimulated (baseline, 0 hr) or stimulated with 0.01 $\mu\text{g/ml}$ unlabeled A2/NY-ESO-1₁₅₇₋₁₆₅ multimers for 6h, 24h and 48h at 37°C under 10 U/ml rhIL-2 media conditions. Following incubation, cells were washed and total RNA was extracted with the miRVana kit (Ambion, Life Technologies), and mature microRNAs (hsa-miR-155, hsa-miR-181a and hsa-

RNU48) were reverse transcribed with the TaqMan MicroRNA Reverse transcription kit (Applied Biosystems). Amplification and real time acquisition were performed using Universal PCR Master Mix (Applied Biosystems) in MicroAmp 384 well plates (Applied Biosystems) on a LightCycler 480 instrument (Roche Ltd.). Ct (RNU48) was subtracted to Ct (miR-155, miR-181a) to calculate relative expression (Δ Ct).

Functional PD-L1 blockade or pharmacological SHP-1/SHP-2 inhibition assays

For PD-L1 blockade, 5×10^5 TCR-transduced CD8⁺ T cells were cultured in 500 μ l RPMI complemented with 8% HS, 150 U/ml rhIL-2 at 37°C without (control) or with 5 μ g/ml PD-L1 blocking antibody (CD274 clone MIH1, eBioscience). Alternatively, 50 μ g/ml sodium stibogluconate (SSG) (Sb content; Santa Cruz Biotechnology, Santa Cruz, CA) was used for SHP-1/SHP-2 inhibition. After 3-4 days, 4×10^5 T cells were incubated at 37°C during 4 hours with 2×10^5 either unloaded T2 (control) or 10 μ M NY-ESO-1-loaded T2 cells (E:T ratio 2:1) together with PE-Cy5 CD107a/LAMP-1 (BD Biosciences) antibody. Acquisition was performed on a LSRI (BD Biosciences) or a Gallios (Beckman Coulter) instrument, and data was analyzed with FlowJo (TreeStar). For target cell killing experiments, TCR-transduced CD8⁺ T cells were incubated with 50 μ g/ml SSG for 3-4 days as described above before assessing antigen-specific lytic activity in a 4-h ⁵¹Cr-release assay against Me 275 cells (HLA-A2⁺/NY-ESO-1⁺) at a 10:1 and 3:1 effector:target (E:T) ratios.

Statistics

For quantitative comparison, paired or unpaired Student's *t* test (2-sample 2-tailed comparison), as indicated, was performed using GraphPad Prism software; $P < 0.05$ was considered as significant.

Study procedure

Human peripheral blood cells were obtained from healthy donors of the Blood Transfusion Center of the University of Lausanne, Switzerland. All donors had previously completed the Swiss National Medical questionnaire, to verify that they fulfilled the criteria for blood donation, and provided written informed consent for the use of blood samples in medical research after anonymization.

ACKNOWLEDGEMENTS

We gratefully acknowledge J. Dudda, P. Guillaume, M. Irving, I. Luescher, R. Perret, B. Salaun and V. Zoete for essential contributions and advice. We are also thankful for the excellent help of N. Montandon, and M. van Overloop. We thank P.O. Gannon for critical reading of the manuscript.

This study was sponsored and supported by the Swiss National Center of Competence in Research (NCCR) Molecular Oncology, the Ludwig Institute for Cancer Research, NY USA, and the Swiss Cancer League grant KLS 2635-08-2010.

REFERENCES

1. Davis, M.M., Krogsgaard, M., Huppa, J.B., Sumen, C., Purbhoo, M.A., Irvine, D.J., Wu, L.C., and Ehrlich, L. 2003. Dynamics of cell surface molecules during T cell recognition. *Annu Rev Biochem* 72:717-742.
2. Schreiber, R.D., Old, L.J., and Smyth, M.J. 2011. Cancer immunoeediting: integrating immunity's roles in cancer suppression and promotion. *Science* 331:1565-1570.
3. Uttenthal, B.J., Chua, I., Morris, E.C., and Stauss, H.J. 2012. Challenges in T cell receptor gene therapy. *J Gene Med* 14:386-399.
4. Stone, J.D., Chervin, A.S., and Kranz, D.M. 2009. T-cell receptor binding affinities and kinetics: impact on T-cell activity and specificity. *Immunology* 126:165-176.
5. Zhao, Y., Bennett, A.D., Zheng, Z., Wang, Q.J., Robbins, P.F., Yu, L.Y., Li, Y., Molloy, P.E., Dunn, S.M., Jakobsen, B.K., et al. 2007. High-affinity TCRs generated by phage display provide CD4+ T cells with the ability to recognize and kill tumor cell lines. *J Immunol* 179:5845-5854.
6. Robbins, P.F., Li, Y.F., El-Gamil, M., Zhao, Y., Wargo, J.A., Zheng, Z., Xu, H., Morgan, R.A., Feldman, S.A., Johnson, L.A., et al. 2008. Single and dual amino acid substitutions in TCR CDRs can enhance antigen-specific T cell functions. *J Immunol* 180:6116-6131.
7. Holler, P.D., Chlewicki, L.K., and Kranz, D.M. 2003. TCRs with high affinity for foreign pMHC show self-reactivity. *Nat Immunol* 4:55-62.
8. Zoete, V., and Michielin, O. 2007. Comparison between computational alanine scanning and per-residue binding free energy decomposition for protein-protein association using MM-GBSA: application to the TCR-p-MHC complex. *Proteins* 67:1026-1047.
9. Zoete, V., Irving, M.B., and Michielin, O. 2010. MM-GBSA binding free energy decomposition and T cell receptor engineering. *J Mol Recognit* 23:142-152.
10. Schmid, D.A., Irving, M.B., Posevitz, V., Hebeisen, M., Posevitz-Fejfar, A., Sarria, J.C., Gomez-Eerland, R., Thome, M., Schumacher, T.N., Romero, P., et al. 2010. Evidence for a TCR affinity threshold delimiting maximal CD8 T cell function. *J Immunol* 184:4936-4946.
11. Irving, M., Zoete, V., Hebeisen, M., Schmid, D., Baumgartner, P., Guillaume, P., Romero, P., Speiser, D., Luescher, I., Rufer, N., et al. 2012. Interplay between T cell receptor binding kinetics and the level of cognate peptide presented by major histocompatibility complexes governs CD8+ T cell responsiveness. *J Biol Chem* 287:23068-23078.
12. Corse, E., Gottschalk, R.A., Krogsgaard, M., and Allison, J.P. 2010. Attenuated T cell responses to a high-potency ligand in vivo. *PLoS Biol* 8.
13. Gonzalez, P.A., Carreno, L.J., Coombs, D., Mora, J.E., Palmieri, E., Goldstein, B., Nathenson, S.G., and Kalergis, A.M. 2005. T cell receptor binding kinetics required for T cell activation depend on the density of cognate ligand on the antigen-presenting cell. *Proc Natl Acad Sci U S A* 102:4824-4829.
14. Kalergis, A.M., Boucheron, N., Doucey, M.A., Palmieri, E., Goyarts, E.C., Vegh, Z., Luescher, I.F., and Nathenson, S.G. 2001. Efficient T cell activation requires an optimal dwell-time of interaction between the TCR and the pMHC complex. *Nat Immunol* 2:229-234.

15. McMahan, R.H., McWilliams, J.A., Jordan, K.R., Dow, S.W., Wilson, D.B., and Slansky, J.E. 2006. Relating TCR-peptide-MHC affinity to immunogenicity for the design of tumor vaccines. *J Clin Invest* 116:2543-2551.
16. Thomas, S., Xue, S.A., Bangham, C.R., Jakobsen, B.K., Morris, E.C., and Stauss, H.J. 2011. Human T cells expressing affinity-matured TCR display accelerated responses but fail to recognize low density of MHC-peptide antigen. *Blood* 118:319-329.
17. Watanabe, N., Gavrieli, M., Sedy, J.R., Yang, J., Fallarino, F., Loftin, S.K., Hurchla, M.A., Zimmerman, N., Sim, J., Zang, X., et al. 2003. BTLA is a lymphocyte inhibitory receptor with similarities to CTLA-4 and PD-1. *Nat Immunol* 4:670-679.
18. Fife, B.T., and Pauken, K.E. 2011. The role of the PD-1 pathway in autoimmunity and peripheral tolerance. *Ann N Y Acad Sci* 1217:45-59.
19. Lorenz, U. 2009. SHP-1 and SHP-2 in T cells: two phosphatases functioning at many levels. *Immunol Rev* 228:342-359.
20. Zhang, Z., Shen, K., Lu, W., and Cole, P.A. 2003. The role of C-terminal tyrosine phosphorylation in the regulation of SHP-1 explored via expressed protein ligation. *J Biol Chem* 278:4668-4674.
21. Stefanova, I., Hemmer, B., Vergelli, M., Martin, R., Biddison, W.E., and Germain, R.N. 2003. TCR ligand discrimination is enforced by competing ERK positive and SHP-1 negative feedback pathways. *Nat Immunol* 4:248-254.
22. Li, Q.J., Chau, J., Ebert, P.J., Sylvester, G., Min, H., Liu, G., Braich, R., Manoharan, M., Soutschek, J., Skare, P., et al. 2007. miR-181a is an intrinsic modulator of T cell sensitivity and selection. *Cell* 129:147-161.
23. Salaun, B., Yamamoto, T., Badran, B., Tsunetsugu-Yokota, Y., Roux, A., Baitsch, L., Rouas, R., Fayyad-Kazan, H., Baumgaertner, P., Devevre, E., et al. 2011. Differentiation associated regulation of microRNA expression in vivo in human CD8+ T cell subsets. *J Transl Med* 9:44.
24. Yi, T., Elson, P., Mitsuhashi, M., Jacobs, B., Hollovary, E., Budd, T.G., Spiro, T., Triozzi, P., and Borden, E.C. 2011. Phosphatase inhibitor, sodium stibogluconate, in combination with interferon (IFN) alpha 2b: phase I trials to identify pharmacodynamic and clinical effects. *Oncotarget* 2:1155-1164.
25. Naing, A., Reuben, J.M., Camacho, L.H., Gao, H., Lee, B.N., Cohen, E.N., Verschraegen, C., Stephen, S., Aaron, J., Hong, D., et al. 2011. Phase I Dose Escalation Study of Sodium Stibogluconate (SSG), a Protein Tyrosine Phosphatase Inhibitor, Combined with Interferon Alpha for Patients with Solid Tumors. *J Cancer* 2:81-89.
26. Pathak, M.K., and Yi, T. 2001. Sodium stibogluconate is a potent inhibitor of protein tyrosine phosphatases and augments cytokine responses in hemopoietic cell lines. *J Immunol* 167:3391-3397.
27. Johnson, L.A., Morgan, R.A., Dudley, M.E., Cassard, L., Yang, J.C., Hughes, M.S., Kammula, U.S., Royal, R.E., Sherry, R.M., Wunderlich, J.R., et al. 2009. Gene therapy with human and mouse T-cell receptors mediates cancer regression and targets normal tissues expressing cognate antigen. *Blood* 114:535-546.
28. Robbins, P.F., Morgan, R.A., Feldman, S.A., Yang, J.C., Sherry, R.M., Dudley, M.E., Wunderlich, J.R., Nahvi, A.V., Helman, L.J., Mackall, C.L., et al. 2011. Tumor regression in patients with metastatic synovial cell sarcoma

- and melanoma using genetically engineered lymphocytes reactive with NY-ESO-1. *J Clin Oncol* 29:917-924.
29. Corse, E., Gottschalk, R.A., and Allison, J.P. 2011. Strength of TCR-peptide/MHC interactions and in vivo T cell responses. *J Immunol* 186:5039-5045.
 30. Dunn, S.M., Rizkallah, P.J., Baston, E., Mahon, T., Cameron, B., Moysey, R., Gao, F., Sami, M., Boulter, J., Li, Y., et al. 2006. Directed evolution of human T cell receptor CDR2 residues by phage display dramatically enhances affinity for cognate peptide-MHC without increasing apparent cross-reactivity. *Protein Sci* 15:710-721.
 31. Valitutti, S. 2012. The Serial Engagement Model 17 Years After: From TCR Triggering to Immunotherapy. *Front Immunol* 3:272.
 32. Zehn, D., Lee, S.Y., and Bevan, M.J. 2009. Complete but curtailed T-cell response to very low-affinity antigen. *Nature* 458:211-214.
 33. Gottschalk, R.A., Hathorn, M.M., Beuneu, H., Corse, E., Dustin, M.L., Altan-Bonnet, G., and Allison, J.P. 2012. Distinct influences of peptide-MHC quality and quantity on in vivo T-cell responses. *Proc Natl Acad Sci U S A* 109:881-886.
 34. Nishimura, H., Okazaki, T., Tanaka, Y., Nakatani, K., Hara, M., Matsumori, A., Sasayama, S., Mizoguchi, A., Hiai, H., Minato, N., et al. 2001. Autoimmune dilated cardiomyopathy in PD-1 receptor-deficient mice. *Science* 291:319-322.
 35. Kroner, A., Mehling, M., Hemmer, B., Rieckmann, P., Toyka, K.V., Maurer, M., and Wiendl, H. 2005. A PD-1 polymorphism is associated with disease progression in multiple sclerosis. *Ann Neurol* 58:50-57.
 36. Prokunina, L., Castillejo-Lopez, C., Oberg, F., Gunnarsson, I., Berg, L., Magnusson, V., Brookes, A.J., Tentler, D., Kristjansdottir, H., Grondal, G., et al. 2002. A regulatory polymorphism in PDCD1 is associated with susceptibility to systemic lupus erythematosus in humans. *Nat Genet* 32:666-669.
 37. Keir, M.E., Butte, M.J., Freeman, G.J., and Sharpe, A.H. 2008. PD-1 and its ligands in tolerance and immunity. *Annu Rev Immunol* 26:677-704.
 38. Yokosuka, T., Takamatsu, M., Kobayashi-Imanishi, W., Hashimoto-Tane, A., Azuma, M., and Saito, T. 2012. Programmed cell death 1 forms negative costimulatory microclusters that directly inhibit T cell receptor signaling by recruiting phosphatase SHP2. *J Exp Med*.
 39. Fowler, C.C., Pao, L.I., Blattman, J.N., and Greenberg, P.D. 2010. SHP-1 in T cells limits the production of CD8 effector cells without impacting the formation of long-lived central memory cells. *J Immunol* 185:3256-3267.
 40. Stromnes, I.M., Fowler, C., Casamina, C.C., Georgopoulos, C.M., McAfee, M.S., Schmitt, T.M., Tan, X., Kim, T.D., Choi, I., Blattman, J.N., et al. 2012. Abrogation of SRC homology region 2 domain-containing phosphatase 1 in tumor-specific T cells improves efficacy of adoptive immunotherapy by enhancing the effector function and accumulation of short-lived effector T cells in vivo. *J Immunol* 189:1812-1825.
 41. Khalil, A.M., Cambier, J.C., and Shlomchik, M.J. 2012. B cell receptor signal transduction in the GC is short-circuited by high phosphatase activity. *Science* 336:1178-1181.
 42. Haasch, D., Chen, Y.W., Reilly, R.M., Chiou, X.G., Koterski, S., Smith, M.L., Kroeger, P., McWeeny, K., Halbert, D.N., Mollison, K.W., et al. 2002.

T cell activation induces a noncoding RNA transcript sensitive to inhibition by immunosuppressant drugs and encoded by the proto-oncogene, BIC. *Cell Immunol* 217:78-86.

43. Pardoll, D., and Drake, C. 2012. Immunotherapy earns its spot in the ranks of cancer therapy. *J Exp Med* 209:201-209.
44. Brahmer, J.R., Tykodi, S.S., Chow, L.Q., Hwu, W.J., Topalian, S.L., Hwu, P., Drake, C.G., Camacho, L.H., Kauh, J., Odunsi, K., et al. 2012. Safety and activity of anti-PD-L1 antibody in patients with advanced cancer. *N Engl J Med* 366:2455-2465.
45. Topalian, S.L., Drake, C.G., and Pardoll, D.M. 2012. Targeting the PD-1/B7-H1(PD-L1) pathway to activate anti-tumor immunity. *Curr Opin Immunol* 24:207-212.

Figure 1. *Functionality, TCR $\alpha\beta$ surface expression levels and TCR/CD8 down-regulation in CD8⁺ T cells engineered with self/tumor-specific TCR of incremental affinities.*

A. Ca²⁺ flux of TCR-transduced CD8⁺ T cells without (baseline) and with 1 μ g/ml HLA-A2/NY-ESO-specific multimer stimulation. Maximal Ca²⁺ flux after ionomycin stimulation indicates equal capacity to mobilize calcium in all T cell variants. **B.** Cytotoxic activity (% of maximal killing) against Me 275 and Me 290 (HLA-A2⁺/NY-ESO-1⁺) and Na8 (HLA-A2⁺/NY-ESO-1⁻) tumor cell lines at an effector target ratio of 10:1. **C.** Percentage of primary CD8⁺ T cells expressing the affinity-optimized NY-ESO-1-specific TCRs as detected by A2/NY-ESO-1₁₅₇₋₁₆₅-specific multimer staining (left panel). Cells with >80% multimer labeling were used for further analysis. Surface expression levels (in MFI) of TCR β -chain BV13.1 (middle) and total $\alpha\beta$ TCR (right) is shown for all CD8⁺ T transduced cells. **D** and **E.** Down-regulation of CD8 coreceptor (**D**; in %) and TCR (**E**; in MFI) in engineered CD8⁺ T cells in the absence (baseline) or presence of 0.1 μ g/ml unlabeled A2/NY-ESO-1-specific multimer. Data from T cells with reduced CD8 expression (**D**; CD8 low) are shown in percent of total T cells (CD8 high and low). TCR down-regulation following stimulation (**E**) is depicted as dark gray histograms or columns.

Figure 2. *Gene expression of CD8⁺ T cells engineered with TCR of incremental affinities.*

A. Microarray hierarchical clustering of gene expression intensities from the 538 gene probes with statistically significant changes in expression values (> 2-fold and adj. P < 0.05) after 6 hr stimulation with unlabeled A2/NY-ESO-1-specific multimer (0.002 µg/ml) separated the samples in two profiles shown above the heatmap. Up-regulated probes are shown in red, down-regulated in blue. Expression profiles of genes from CD8⁺ T cells transduced with either very low (V49I) or very high (wtc51m) affinity TCRs, after 6 hr stimulation (names depicted in red) cluster together within the unstimulated (0 hr) profile 1 group. **B.** 524 genes enriched between 0 hr and 6 hr in T cells transduced with TCRs giving maximal function (G50A, A97L, DMβ, TMβ) could be classified using GOTermFinder. **C.** Log₂-fold-changes in the expression level of representative TCR response genes (*CRTAM*, *IL2RA*), T cell effector cytokine (*IFNG*) and costimulatory molecules (*TNFRSF18* (*GITR*), *TNFRSF4* (*OX40*), *TNFRSF9* (*4-1BB*)).

Figure 3. *Levels of ZAP-70 and ERK 1/2 phosphorylation in SUP-T1 and CD8⁺ T cells engineered with TCRs of incremental affinities.*

A and C. TCR-transduced SUP-T1 T cells (**A**) and CD8⁺ T cells (**C**) were stimulated with 10 µg/ml A2/NY-ESO-1₁₅₇₋₁₆₅ multimers at 37°C for the indicated time-points. Total ZAP-70 and ERK 1/2 are shown as internal controls, while α-tubulin (**A**) or actin (**C**) expression levels were used as loading controls between samples. Data are each representative of three independent experiments. TCR-untransduced cells (Ø). For CD8⁺ T cells, all lines were run on the same gel but were noncontiguous. **B.** To allow direct comparison between the different SUP-T1 transduced TCR variants, intensity of ZAP-70 and ERK1/2 phosphorylation levels were quantified and normalized to α-tubulin. Data from three independent experiments are presented as min-to-max bar graphs with average mean lines.

Figure 4. *Surface expression of costimulatory molecules and co-activatory/inhibitory receptors in CD8⁺ T cells engineered with TCR of incremental affinities.*

A. Surface expression levels of the TNFR-TNFR ligand pairs (i) CD27-CD70 and (ii) HVEM-BTLA as well as of CD28 and CD8 β are shown in steady-state conditions (unstimulated cells). TCR variants are presented in order of increased affinity. Data were obtained from ten independent experiments. **B.** Baseline expression levels of Granzyme B and Perforin in CD8⁺ T cells transduced with TCR variants. Data were obtained from 7 independent experiments. **A and B.** Unpaired two-tailed *t* test; *** P < 0.001; ** 0.001 < P < 0.01; * 0.01 < P < 0.05; ns, not significant.

Figure 5. *PD-1 expression in TCR-engineered CD8⁺ T cells and functional impact of PD-L1 blockade.*

A. Unstimulated at baseline (0h) and Log₂ fold change (0-6 hr) expression levels of *PD1* transcripts as detected in microarray analysis. **B.** Average surface expression of PD-1 (n > nine independent experiments) and its ligand PD-L1 (n > six independent experiments) of TCR-engineered CD8⁺ T. Unpaired two-tailed *t* test; *** P < 0.001; ** 0.001 < P < 0.01. **C.** Representative histograms of PD-1 surface expression (in MFI) in TCR-engineered CD8⁺ T cells under steady-state conditions. **D.** Representative histograms of the levels (in MFI) of the degranulation marker LAMP-1/CD107a in TCR-transduced CD8⁺ T cells without (control, blue histograms) or with PD-L1 blocking antibody (red histograms) prior to 4 hr stimulation with 10 μM NY-ESO-1₁₅₇₋₁₆₅-loaded T2 cells. CD107a degranulation following stimulation with unloaded T2 cells is depicted as gray histograms. Graphs below each respective histogram represent the direct comparison of TCR stimulation-associated CD107a levels without (-) or with PD-L1 blockade (+). Data were obtained from more than four independent experiments. Paired two-tailed *t* test, ** 0.001 < P < 0.01. **E.** Relative CD107a degranulation ratio (in gMFI) obtained in the presence versus the absence of PD-L1 blocking antibody. Graphs are depicted as relative CD107 fold-increase following stimulation with unloaded (left panel) or NY-ESO-1-pulsed (right panel) T2 cells. Unpaired two-tailed *t* test; ** 0.001 < P < 0.01; * 0.01 < P < 0.05; ns, not significant.

Figure 6. Levels of SHP-1 protein and of miR-155 and miR-181a expression in CD8⁺ T cells engineered with TCRs of incremental affinities.

A. Unstimulated at baseline (0h) and Log₂ fold change (0-6 hr difference) expression levels of *SHP1* transcripts as detected in microarray analysis. **B and C.** TCR-transduced CD8⁺ T cells (**B**) and SUP-T1 cells (**C**) were stimulated with 10 µg/ml A2/NY-ESO-1₁₅₇₋₁₆₅ multimers for the indicated time-points and assessed for SHP-1 phosphorylation and total SHP-1 levels by Western blotting. Actin (**B**) or α-tubulin (**C**) expression levels were used as loading controls between samples. Data are each representative of three independent experiments. For CD8⁺ transduced T cell samples, all lines were run on the same gel, but were noncontiguous. TCR-untransduced; Ø. **D.** To allow direct comparison between the engineered SUP-T1 cells, intensity of SHP-1 phosphorylation and of total SHP-1 levels were quantified and normalized to α-tubulin (n = 3 independent experiments). **E.** Expression levels of miR-181a and miR-155 were determined by qRT-PCR in TCR-transduced CD8⁺ T cells following stimulation with 0.1µg/ml A2/NY-ESO-1₁₅₇₋₁₆₅ multimers at the indicated time-points. Data represent relative expression compared to RNU48 control and are representative of three independent experiments. Pri-miR-155 (BIC) mRNA expression values (inset) were retrieved from the microarray analysis.

Figure 7. *Pharmacological inhibition of SHP-1 phosphatase in TCR engineered CD8⁺ T cells*

A. Representative histograms of the levels (in MFI) of LAMP-1/CD107a expression in TCR-transduced CD8⁺ T cells without (control, blue histograms) or with SHP-1 inhibition by SSG (red histograms) prior to 4 hr stimulation with 10 μ M NY-ESO-1₁₅₇₋₁₆₅-loaded T2 cells. CD107a degranulation following stimulation with unloaded T2 cells is depicted as gray histograms. Graphs below each respective histogram represent the direct comparison of TCR stimulation-associated CD107a levels without (-) or with SHP-1 inhibition (+). Paired two-tailed *t* test; *** $P < 0.001$; ** $0.001 < P < 0.01$; * $0.01 < P < 0.05$. Data were obtained from six independent experiments. **B.** Relative CD107a degranulation ratio (in gMFI) obtained in the presence versus the absence of SHP-1 inhibition compound SSG. Graphs show relative CD107 fold-increase following stimulation with unloaded (left panel) or NY-ESO-1-pulsed (right panel) T2 cells. **C.** Melanoma cell killing by TCR-transduced CD8⁺ T cells without (mock) or with SSG treatment for 4 days. Tumor reactivity for the melanoma cell line Me 275 was assessed in a functional 4h ⁵¹Cr release assay. **D.** Relative ⁵¹Cr count-per-minute (CPM) ratio with and without SSG at the indicated E:T ratios. Unpaired two-tailed *t* test; *** $P < 0.001$; ** $0.001 < P < 0.01$; * $0.01 < P < 0.05$; ns, not significant.

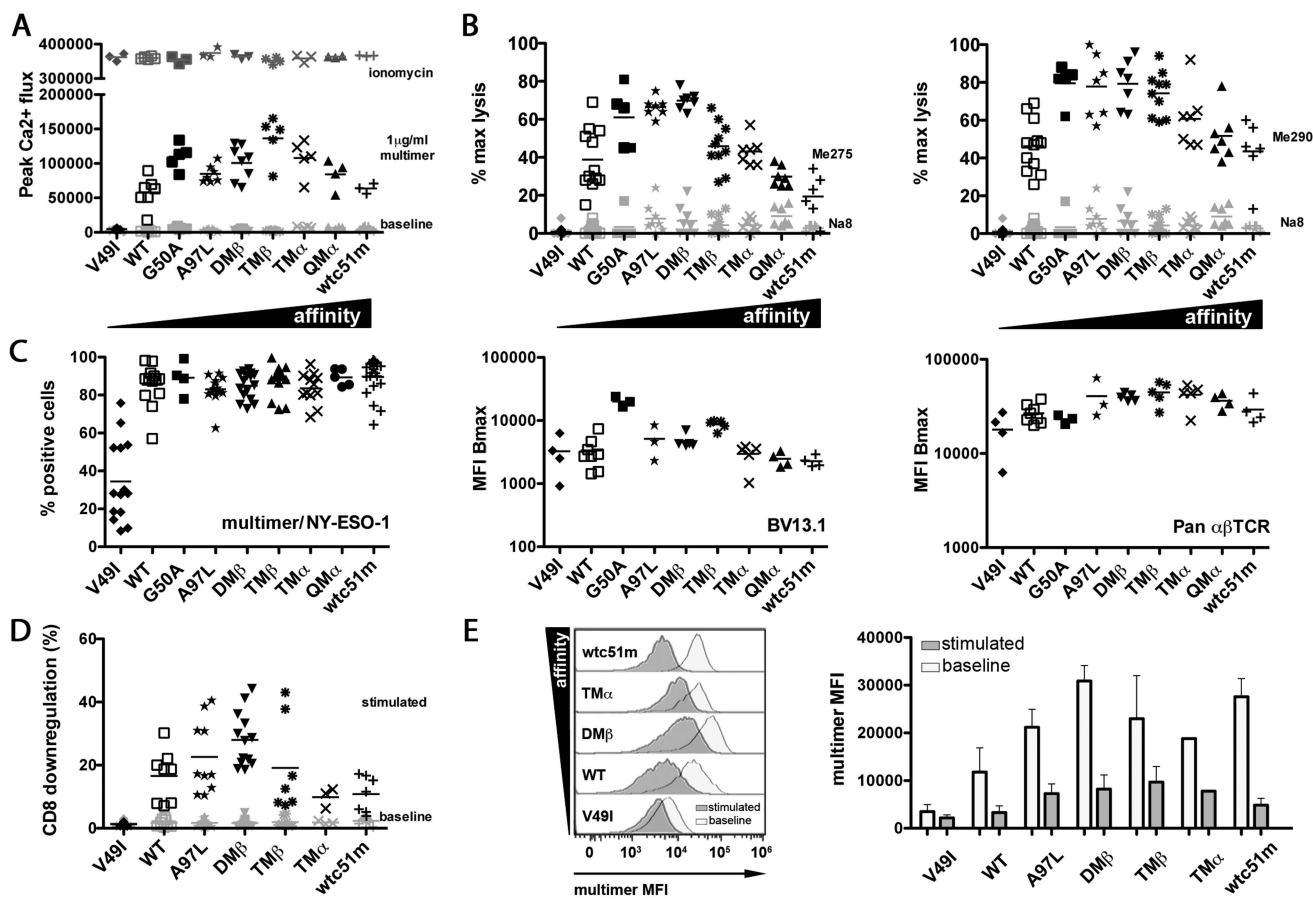


Figure 1
Hebeisen et al.

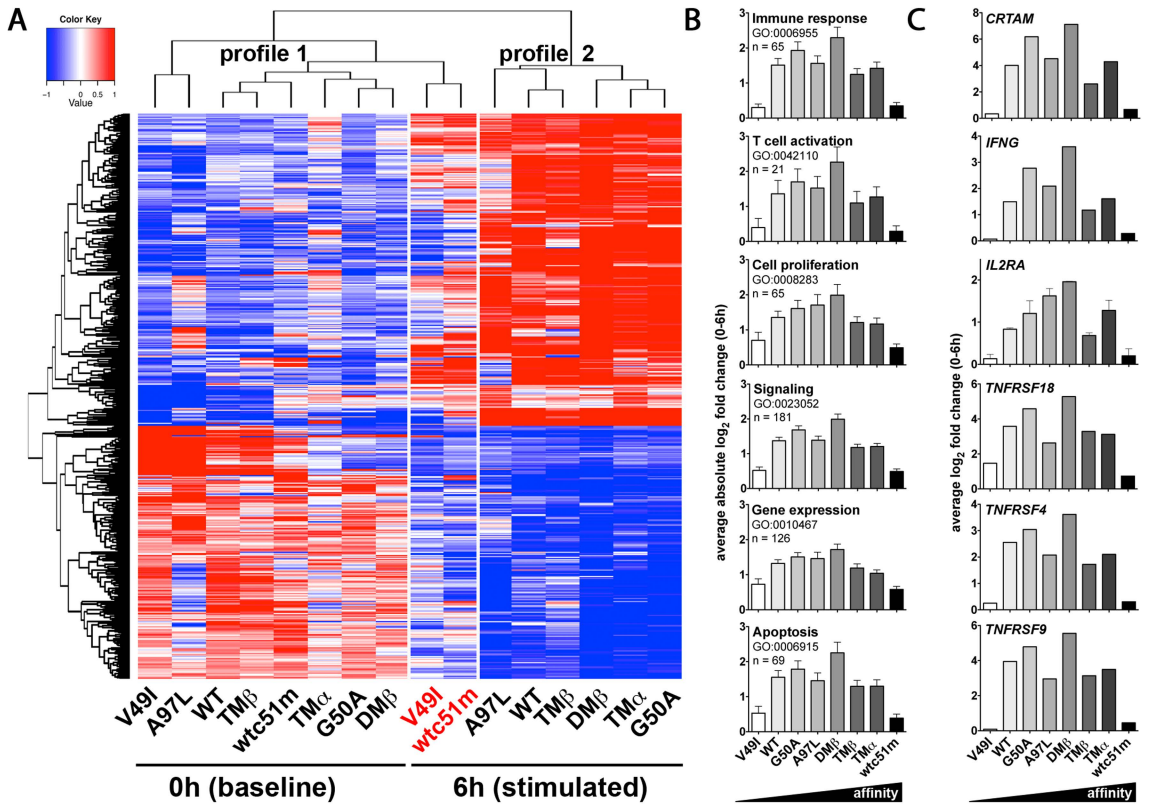


Figure 2
Hebeisen et al.

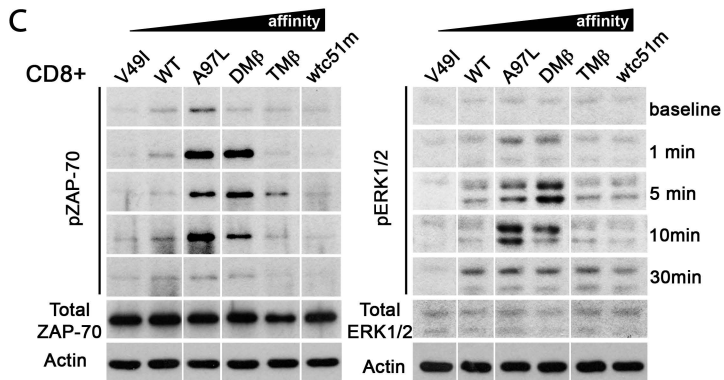
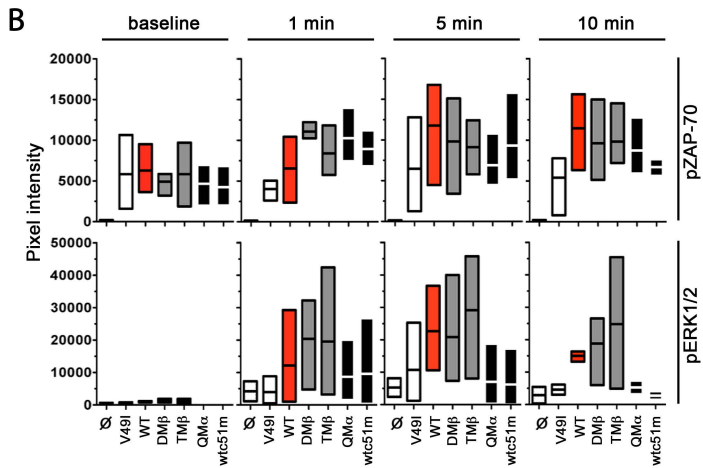
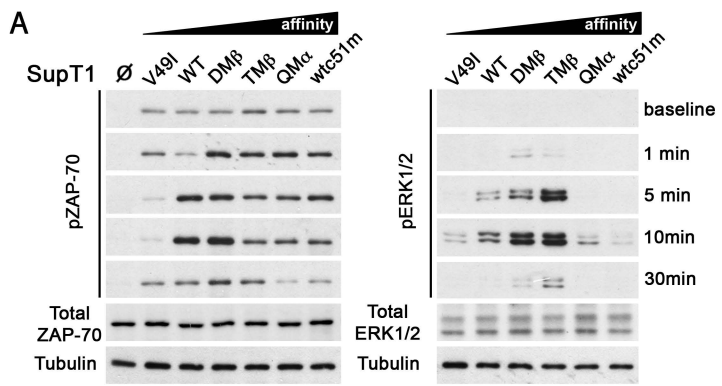


Figure 3
Hebeisen et al.

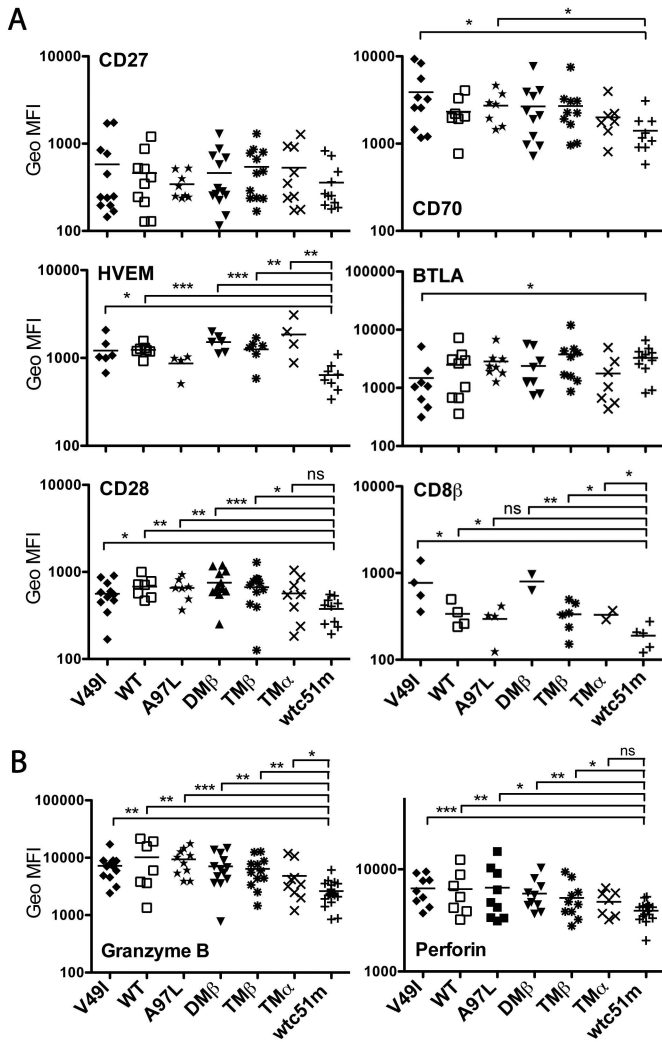


Figure 4
Hebeisen et al.

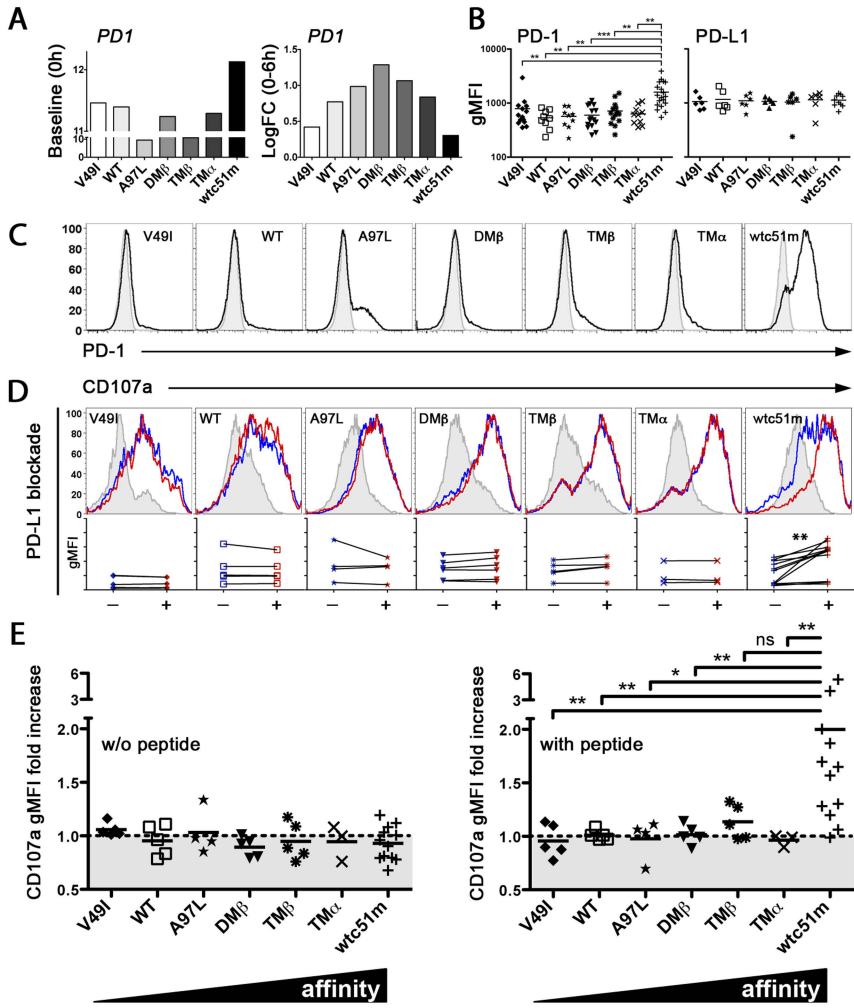


Figure 5
Hebeisen et al.

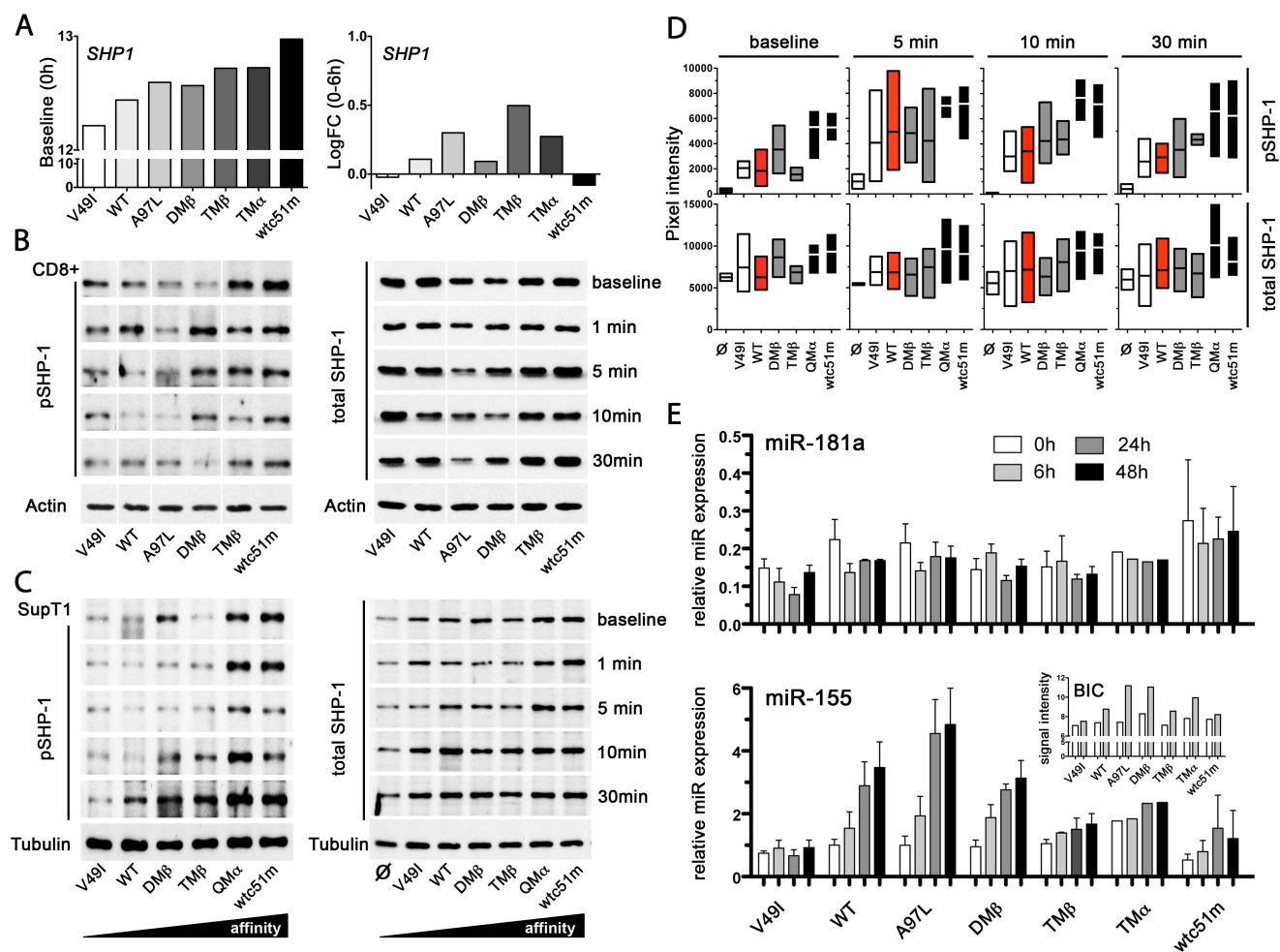


Figure 6
Hebeisen et al.

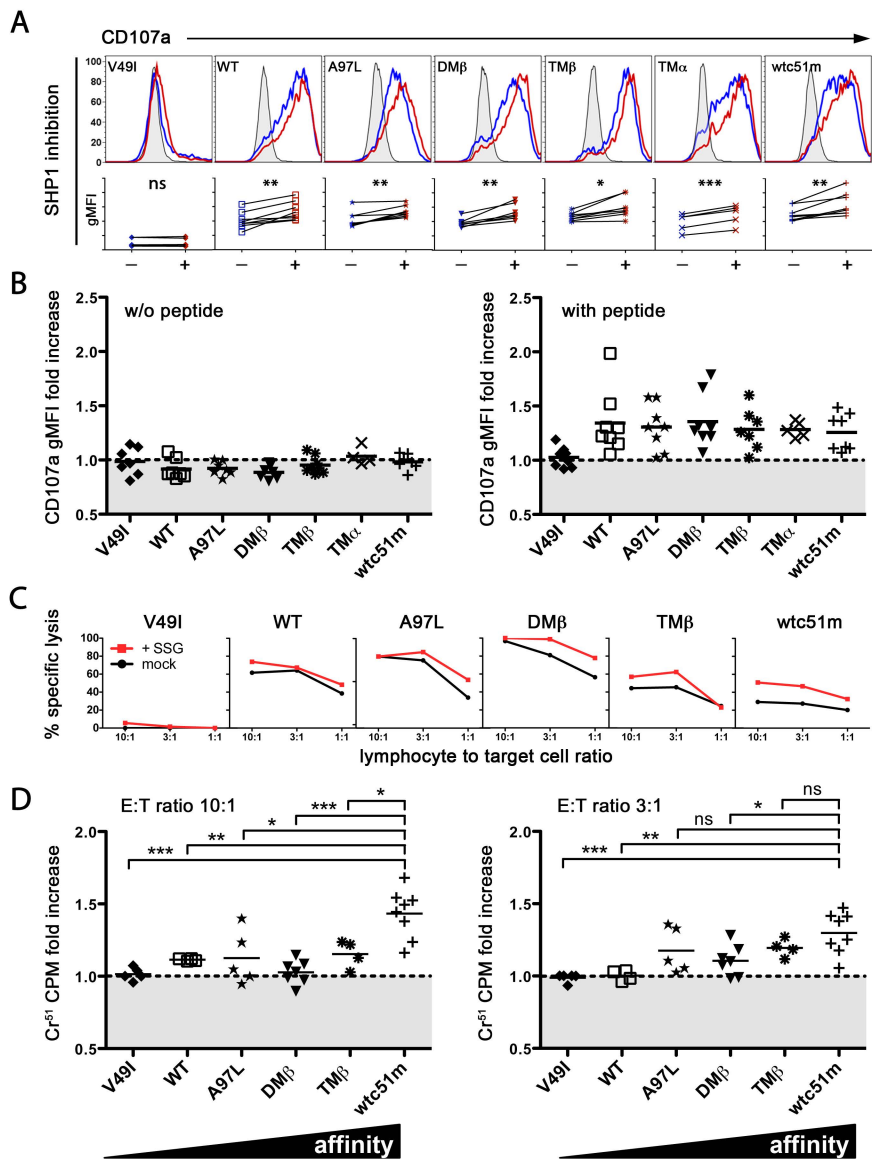


Figure 7
Hebeisen et al.

SUPPLEMENTAL METHODS*Flow cytometry immunofluorescence analysis*

The following fluorophore-conjugated antibodies were used for staining of surface costimulatory molecules and co-activatory/inhibitory receptors for 20 min at 4°C; CD27 (APC-Alexa780; eBioscience), CD70 (FITC; BD Biosciences), HVEM (APC; Biolegend), BTLA (PE; BD Biosciences), CD28 (FITC; BD Biosciences), CD8 α (PerCP-Cy5.5; Biolegend), CD8 β (PE; Beckman Coulter), PD-1 (PerCP-eF1710; eBioscience), PD-L1 (PE-Cy7; BD Bioscience), PD-L2 (APC; Biolegend), Granzyme B (FITC; Biolegend) and Perforin (APC, Biolegend). Appropriate isotype controls were used to define negative populations.

Calcium flux assays upon NY-ESO-1 peptide loaded T2 cells

15x10⁴ T2 cells pulsed with increasing concentrations of NY-ESO₁₅₇₋₁₆₅ peptide were used as APCs and brought in contact with 5x10⁴ (E:T ratio 1:3), 2 μ M Indo1-AM loaded TCR-transduced primary CD8⁺ T cells through a 10 seconds 1400 rpm centrifugation before immediate cytometric recording. Intracellular Ca²⁺ flux was recorded under UV excitation and constant temperature of 37°C using a thermostat device on a LSR II SORP (BD Biosciences) flow cytometer. Indo-1(violet)/Indo-1(blue) 405/525 nm emission ratio was analyzed by FlowJo kinetics module software (TreeStar).

Microarray analysis

Total RNA was isolated using NucleoSpin® RNA II extraction protocols (Macherey-Nagel, Bietlenheim, Germany) and RNA was of high quality and integrity, as verified through Agilent 2100 Bioanalyser platform (Agilent Technologies, Waldbronn, Germany). 1 μ g of RNA was used for T7-based amplification and Cy3 labeling. Samples were hybridized to Agilent Whole Human Genome Oligo Microarrays 4x44K and scanned using the Agilent microarray scanner system (Agilent). The Agilent Feature Extraction Software was used for readout and processing of image

files. Background correction, filtering of data, and quantile normalization were done using R and the *Agi4x44PreProcess* software package as described in the package manual. The Limma software package was used to identify differentially expressed genes and to calculate the \log_2 fold change. Gene probes were considered significant if their P value corrected for a FDR of 0.05 was $P < 0.05$. Fold change expression between 0 hr and 6 hr detected in T cells variants generating optimal function (G50A, A97L, DM β and TM β) were converted into UniProt IDs using BioMart and then classified into broad gene ontology (GO) terms using the GOTermFinder (<http://go.princeton.edu/cgi-bin/GOTermFinder>). The \log_2 fold changes of probes assigned to the same GO-term were averaged in absolute value to yield a general measure of expression change independent of its direction.

SUPPLEMENTAL FIGURE LEGENDS

Supplemental Figure 1. *Calcium mobilization assays in primary CD8⁺ T cells engineered with affinity-optimized TCR variants*

A. A representative kinetic analysis of Ca²⁺ mobilization in CD8⁺ T cells transduced with affinity-optimized TCR variants after stimulation with T2 cells (APC) loaded with increasing peptide concentrations. Acquisition of Ca²⁺ influx was performed over time in the following order: (i) without APC, (ii) with APC loaded with increasing concentrations of NY-ESO-1₁₅₇₋₁₆₅ peptide (from 0 to 5 μM) and (iii) with ionomycin as a positive control. **B.** The mean Ca²⁺ influx values for all independent experiments (n > 3) for each engineered CD8⁺ T cells following stimulation at the indicated peptide concentration (no peptide, 0.001 to 1 μM). Ca²⁺ mobilization obtained after stimulation with NY-ESO-1-expressing Me 290 or Me 275 (HLA-A2⁺/NY-ESO⁺) tumor cell lines in TCR WT-transduced T cells are highlighted as a shaded gray box on the graphs, and indicate that the 0.01 μM peptide-loaded T2 stimulation condition resembles closely to the natural antigen presentation by tumor cell lines. Of note, no Ca²⁺ flux is detected upon stimulation of untransduced CD8⁺ T cells (no TCR) or upon stimulation of WT NY-ESO-1-transduced T cells with Flu-specific peptide (WT/Flu). Maximal Ca²⁺ flux after ionomycin stimulation indicates equal capacity to mobilize calcium in all T cell variants. Importantly, similar data were obtained independently of stimulation with either peptide-pulsed APCs (as shown here) or directly with A2/peptide multimers (Figure 1A, see main manuscript).

Supplemental Figure 2. *Surface levels of TCR expression and TCR/CD8 down-regulation in engineered SUP-T1 and CD8⁺ T cells*

A. Percentage of SUP-T1 cells expressing affinity-optimized NY-ESO-1-specific TCRs as detected by NY-ESO-1₁₅₇₋₁₆₅-specific multimer staining (left panel). Surface expression levels (in MFI) of TCR β -chain BV13.1 (middle) and total $\alpha\beta$ TCR (right) are shown for all SUP-T1 transduced cells. **B.** Surface staining of CD8 and TCR β -chain BV13.1 on CD8⁺ T cells engineered with TCR variants in the absence (unstimulated) or following stimulation with 0.1 μ g/ml unlabeled HLA-A2/NY-ESO-1₁₅₇₋₁₆₅ specific multimers for 4 hours. Representative dot-plots showing the proportion of reduced CD8 expression (CD8 low) compared to CD8 high expression for all engineered T cells. Of note, increased CD8 down-modulation was observed for T cells expressing optimal TCR affinities (e.g. A97L, DM β and TM β), in contrast to supraphysiological T cells (e.g. TM α , wtc51m). **C and D.** Down-regulation of TCR expression on engineered CD8⁺ T cells was assessed in the absence (-) or presence (+) of 10 μ M peptide-loaded T2 (**C**) or 0.1 μ g/ml unlabeled A2/ NY-ESO-1₁₅₇₋₁₆₅ specific multimers (**D**) for 4 hours. TCR down-regulation was revealed by reduced multimer fluorescence (**C**) or TCR β -chain BV13.1 staining (**D**). Importantly, similar results were obtained independently following stimulation with either peptide-pulsed T2 cells (Supplemental Fig. 2C) or A2/peptide multimers (Figure 1E, main manuscript).

Supplemental Figure 3. *Global gene expression profiles of CD8⁺ T cells engineered with affinity-optimized TCR variants*

A genome-wide microarray analysis was performed on primary CD8⁺ T cells expressing TCR variants following low dose (0.002 µg/ml) of HLA-A2/ NY-ESO-1₁₅₇₋₁₆₅ specific multimer stimulation as described in the main manuscript. We identified 524 genes enriched between 0 hr and 6 hr in T cells transduced with optimal TCR variants (G50A, A97L, DMβ, TMβ), which could be further classified according to GO terms (Figure 2, main manuscript). Using the same list of enriched genes, we also assessed the average log₂ gene expression variance for each engineered T cell variant at baseline (un-stimulated) and per GO term. Variance is defined as the difference from the mean on a log₂ scale. These results show that in contrast to stimulated CD8⁺ T cells, no major changes in the GO terms (immune response, T cell activation, cell proliferation, signaling, gene expression and apoptosis) were observed within un-stimulated T cells and among the various TCR-transduced T cells. However, it should be noted that a marginal trend in gene expression over-representation was sometimes found for the T cells bearing highest TCR affinities (e.g. TMα and wtc51m). Moreover, we also noticed small fluctuations, particularly when we compared the T cell variants for the GO term “gene expression” and “cell proliferation”, likely reflecting differences in culture conditions occurring during the expansion of these cells before performing the micro-array experiments.

Supplemental Figure 4. *Levels of ZAP-70 and ERK 1/2 protein expression and phosphorylation in engineered T cells with affinity-optimized TCR variants*

A. TCR-transduced SUP-T1 T cells and CD8⁺ T cells were stimulated with 10 µg/ml HLA-A2/NY-ESO-1₁₅₇₋₁₆₅ multimers at 37°C for the indicated time-points and assessed for total ZAP-70 and total ERK1/2 levels by Western blotting, in parallel to the data presented in Figure 3A and C (main manuscript). Tubulin (SUP-T1) or actin (CD8⁺) expression levels were used as loading controls between samples and time-points. TCR-untransduced cells; Ø. n.d., not done. **B.** To allow direct comparison between TCR-engineered SUP-T1 cells, intensity of total ZAP-70 and total ERK1/2 levels were quantified and normalized to α-tubulin. Data from 3 independent experiments are presented as min-to-max bar graphs with average mean lines. TCR variants are presented in order of increased affinity. Baseline represents the unstimulated T cells. **C.** Example of another representative western blot analysis on stimulated CD8⁺ T cells. ZAP-70 and ERK1/2 phosphorylation levels as well as total ZAP-70 and ERK1/2 are depicted at the indicated time-points following antigen-specific stimulation.

Supplemental Figure 5. *Levels of SHP-1 phosphorylation and of total SHP-2 protein expression in engineered T cells with affinity-optimized TCR variants*

A. Actin (for CD8⁺ T cells) or α -tubulin (for SUP-T1 cells) expression levels were used as loading controls between samples and time-points, and were performed in parallel to the data presented in Figure 6B and C (main manuscript). **B.** TCR-transduced CD8⁺ T cells and SUP-T1 cells were stimulated with 10 μ g/ml HLA-A2/NY-ESO-1₁₅₇₋₁₆₅ multimers at 37°C for the indicated time-points and assessed for SHP-1 phosphorylation levels. TCR-untransduced cells; \emptyset . **C.** Un-stimulated at baseline (0h) and Log₂ fold change (0-6 hr difference) expression levels of *SHP2* transcripts as detected in microarray analysis. **D and E.** TCR-transduced CD8⁺ T cells (**D**) and SUP-T1 cells (**E**) were stimulated with 10 μ g/ml A2/NY-ESO-1₁₅₇₋₁₆₅ multimers for the indicated time-points and assessed for total SHP-2 protein expression levels by Western blotting. We used for SHP-2 protein expression analysis the following antibody: rabbit anti-SHP-2 (C-18) (Santa Cruz Biotechnology, Inc). Actin (for CD8⁺ T cells) or α -tubulin (for SUP-T1 cells) expression levels were used as loading controls between samples. Baseline represents the un-stimulated T cells. For CD8⁺ transduced T cell samples, all lines were run on the same gel, but were noncontiguous.

Supplemental Table 1. Relative affinities of the sequence-optimized A2/NY-ESO-1 specific TCR variants

TCR AV23.1-BV13.1 ^a	CDR modification	Relative affinity ^b
wtc51m ^c	CDR2 β	1427
QM α	CDR2+3 β ; CDR2 α	153
TM α	CDR2 β ; CDR2 α	54
TM β	CDR2+3 β	24
DM β	CDR2 β	11
A97L	CDR3 β	8
G50A	CDR2 β	5
WT ^d	none	1
V49I	CDR2 β	N/A

^aThe NY-ESO-1-specific TCR AV23.1-BV13.1 was optimized by in silico modeling, through amino acid substitutions in CDR2 α and/or CDR2 β and/or CDR3 β loops as previously described (1).

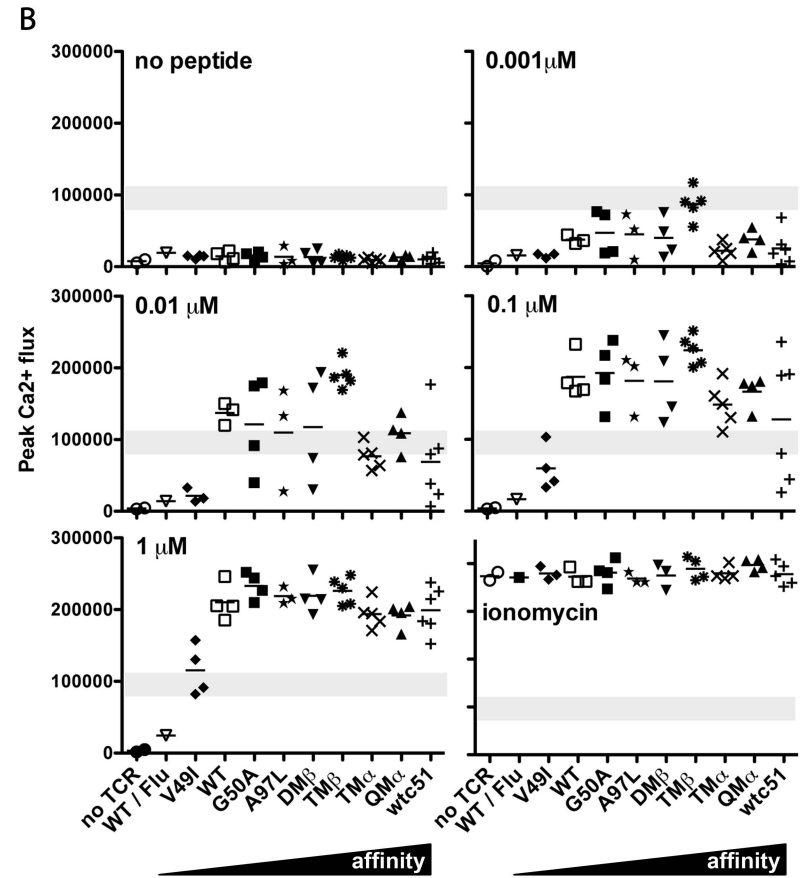
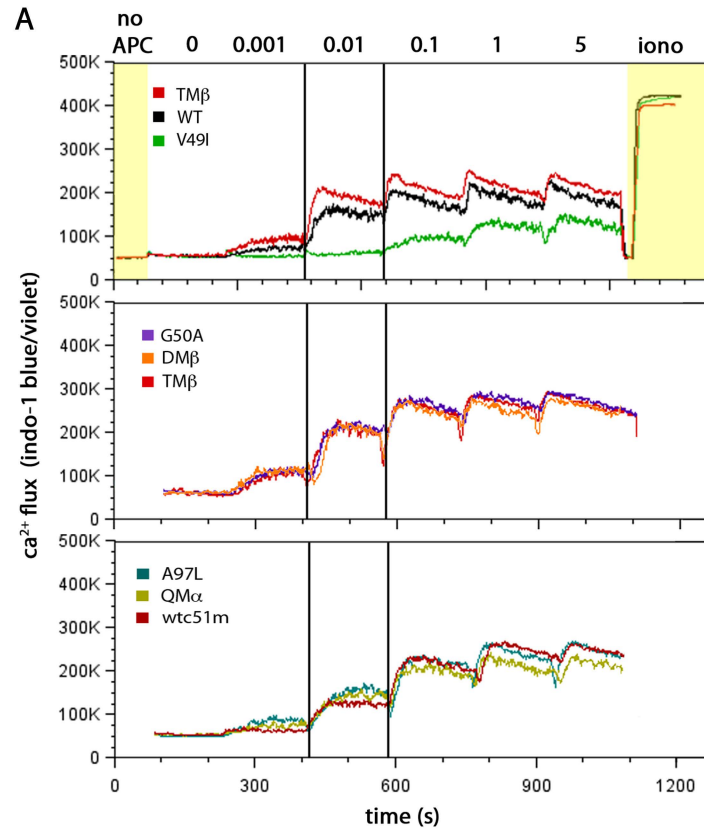
^bSequence-optimized TCR affinities are indicated in relative fold-increase from the WT TCR (K_D , 21.4 μ M), as characterized recently (2). A sub-physiological, weak-binding TCR (V49I), with an estimated affinity of > 100 μ M to pMHC was included. N/A, not applicable.

^cThe modified wtc51 TCR variant, comprises the WT TCR sequences with four amino acid replacements within the CDR2 β loop (3), resulting in the drastic increase of its affinity towards pMHC.

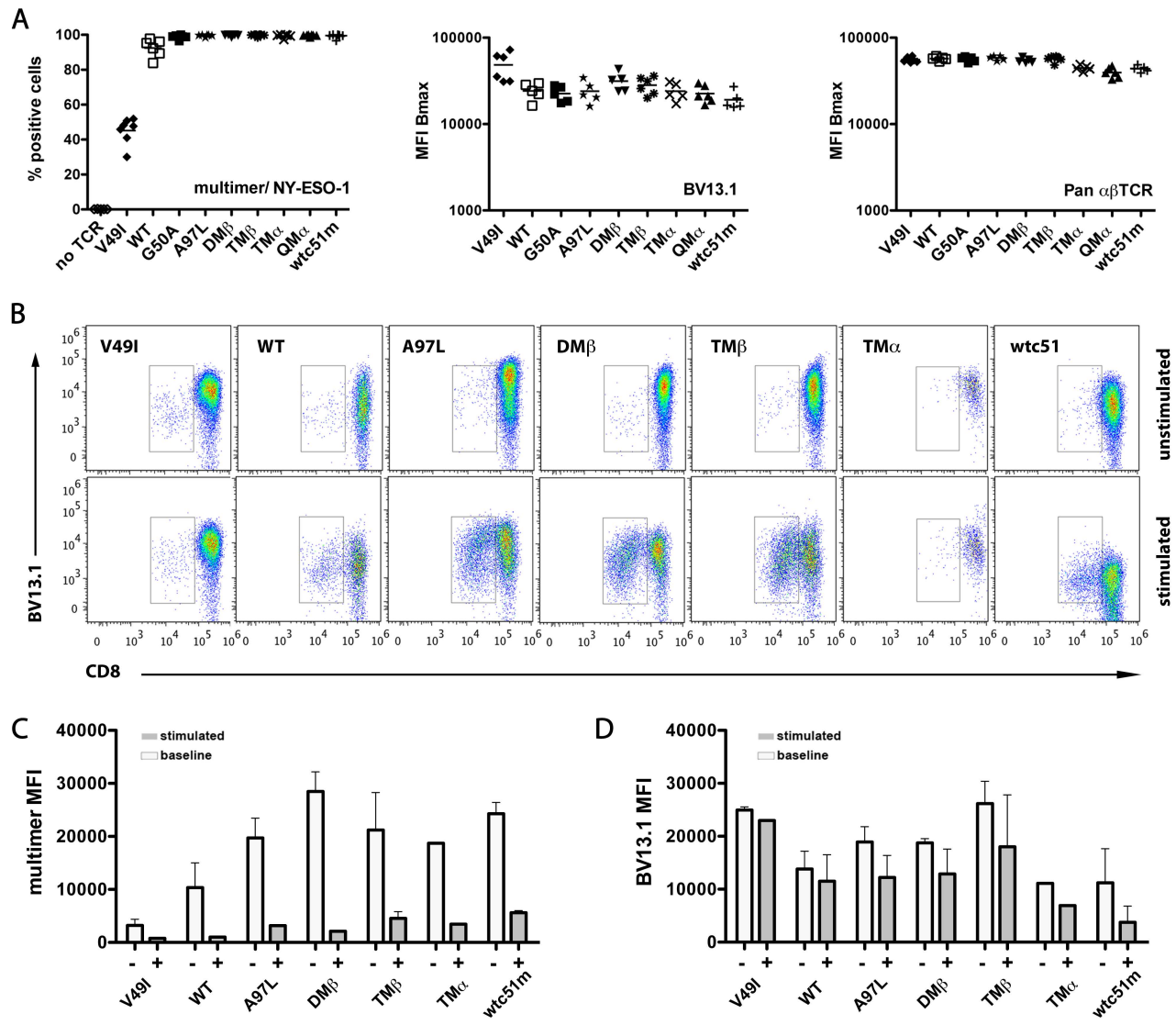
^dWild-type (WT) TCR isolated from melanoma patient LAU 155 (4).

SUPPLEMENTAL REFERENCES

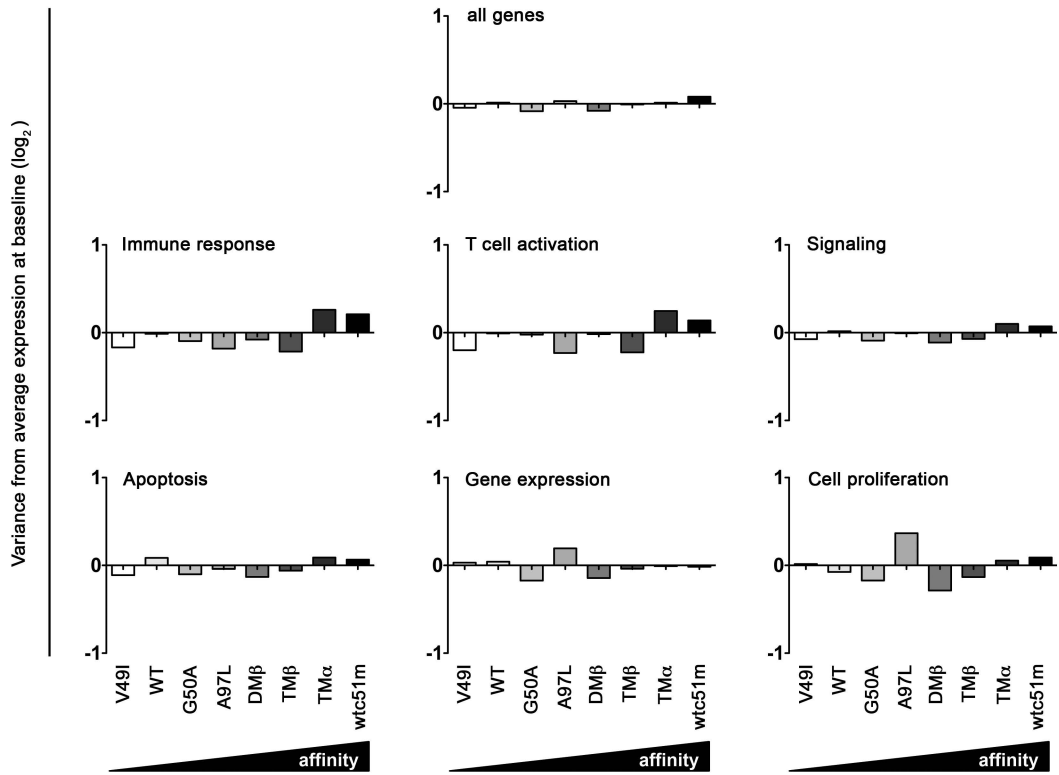
1. Zoete, V., Irving, M.B., and Michielin, O. 2010. MM-GBSA binding free energy decomposition and T cell receptor engineering. *J Mol Recognit* 23:142-152.
2. Irving, M., Zoete, V., Hebeisen, M., Schmid, D., Baumgartner, P., Guillaume, P., Romero, P., Speiser, D., Luescher, I., Rufer, N., et al. 2012. Interplay between T cell receptor binding kinetics and the level of cognate peptide presented by major histocompatibility complexes governs CD8+ T cell responsiveness. *J Biol Chem* 287:23068-23078.
3. Dunn, S.M., Rizkallah, P.J., Baston, E., Mahon, T., Cameron, B., Moysey, R., Gao, F., Sami, M., Boulter, J., Li, Y., et al. 2006. Directed evolution of human T cell receptor CDR2 residues by phage display dramatically enhances affinity for cognate peptide-MHC without increasing apparent cross-reactivity. *Protein Sci* 15:710-721.
4. Derre, L., Bruyninx, M., Baumgaertner, P., Ferber, M., Schmid, D., Leimgruber, A., Zoete, V., Romero, P., Michielin, O., Speiser, D.E., et al. 2008. Distinct sets of alphabeta TCRs confer similar recognition of tumor antigen NY-ESO-1157-165 by interacting with its central Met/Trp residues. *Proc Natl Acad Sci U S A* 105:15010-15015.



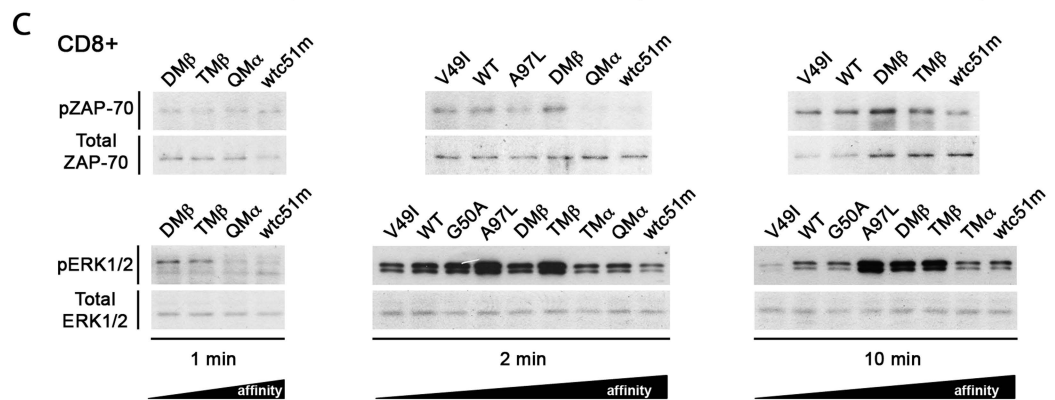
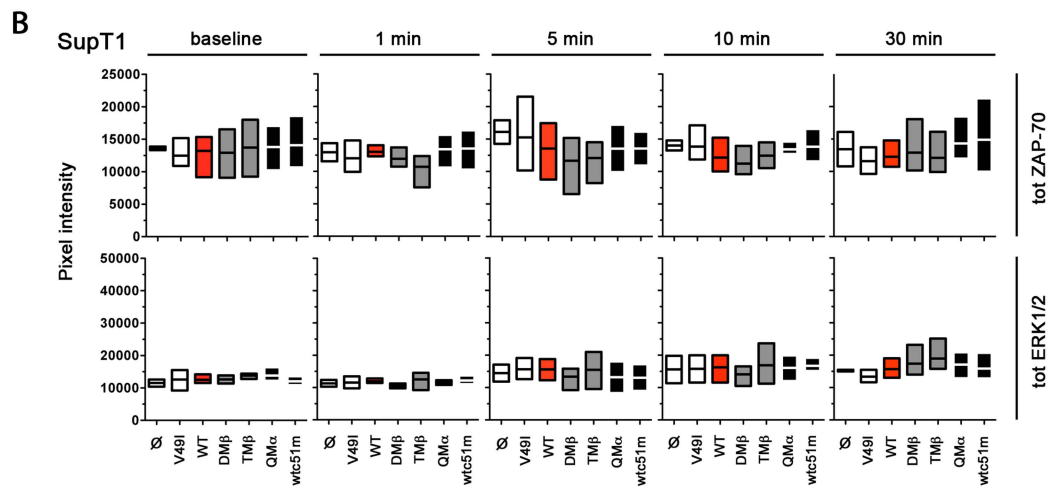
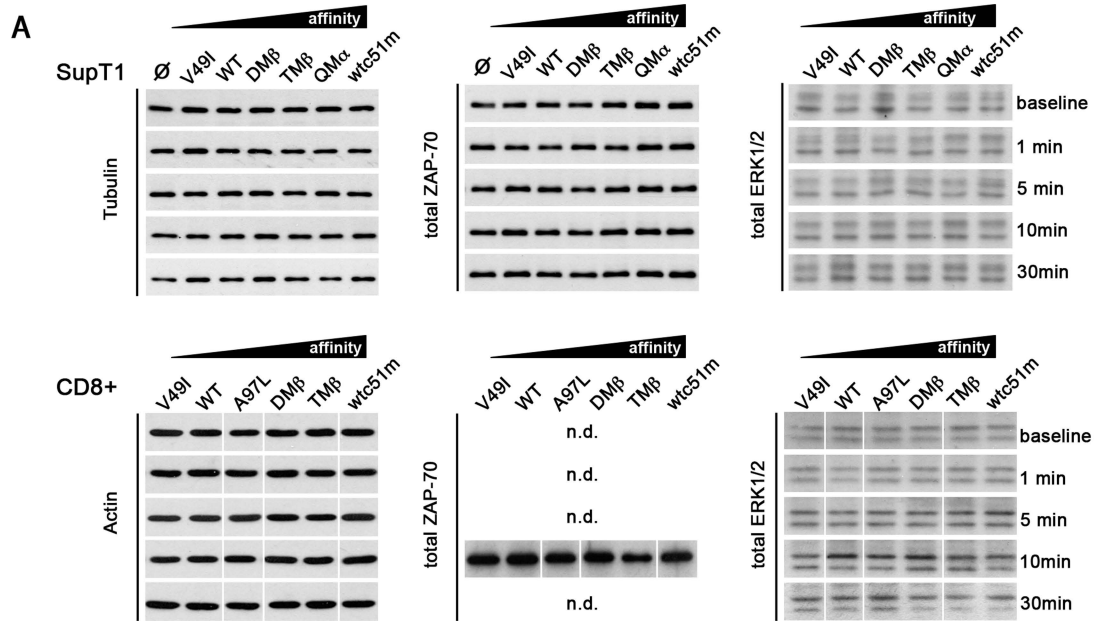
Supplemental Figure 1
Hebeisen et al.



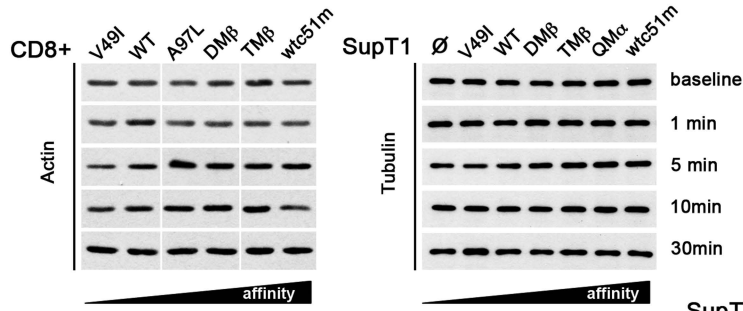
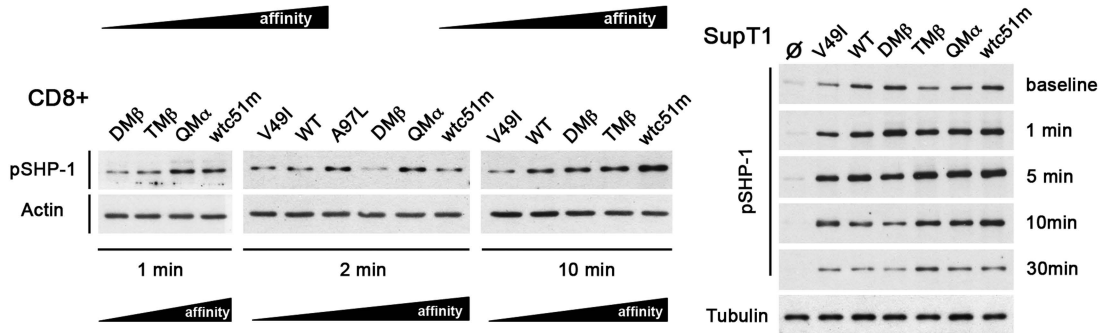
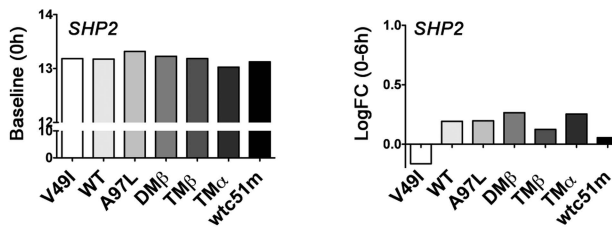
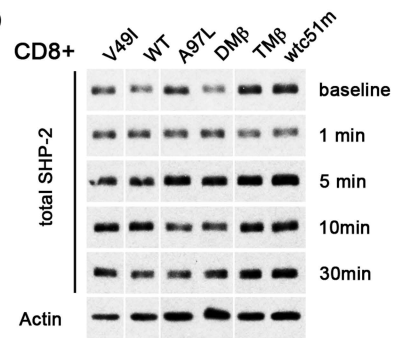
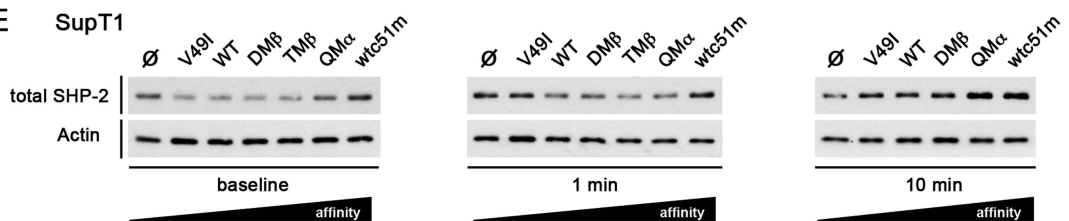
Supplemental Figure 2
Hebeisen et al.



Supplemental Figure 3
Hebeisen et al.



Supplemental Figure 4
Hebeisen et al.

A**B****C****D****E**

Supplemental Figure 5
Hebeisen et al.